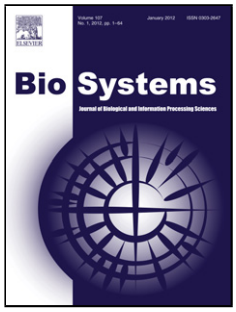

Title: A General Framework Dedicated to Computational Morphogenesis Part I - Constitutive equations

Authors: Pridi Siregar, Nathalie Julen, Peter Hufnagl, George Mutter

PII: S0303-2647(18)30073-X
DOI: https://doi.org/10.1016/j.biosystems.2018.07.003
Reference: BIO 3860

To appear in: *BioSystems*

Received date: 24-2-2018
Revised date: 30-5-2018
Accepted date: 5-7-2018

Please cite this article as: Siregar P, Julen N, Hufnagl P, Mutter G, A General Framework Dedicated to Computational Morphogenesis Part I - Constitutive equations, *BioSystems* (2018), https://doi.org/10.1016/j.biosystems.2018.07.003

A General Framework Dedicated to Computational Morphogenesis

Part I - Constitutive equations

Pridi Siregar[1], Nathalie Julen[1], Peter Hufnagl[2] & George Mutter[3]

[1] Integrative BioComputing - IBC, Chantepie, France

[2] Department of Digital Pathology and IT, Institute of Pathology, Charité – Universitätsmedizin Berlin, Berlin, Germany

[3] Department of Pathology, Harvard Medical School and Brigham and Women's Hospital, Boston, MA, USA

*Corresponding author at: Integrative BioComputing IBC, Centre d'Affaires Buro Club, Place du Granier, 35135 Chantepie, France.
email: pridi.siregar@ibiocomputing.com (P. Siregar).

Content

Abstract

In order to understand living organisms, considerable experimental efforts and resources have been devoted to correlate genes and their expressions with cell, tissue, organ and whole organisms' phenotypes. This data driven approach to knowledge discovery has led to many breakthrough in our understanding of healthy and diseased states, and is paving the way to improve the diagnosis and treatment of diseases. Complementary to this data-driven approach, computational models of biological systems based on first principles have been developed in order to deepen our understanding of the multi-scale dynamics that drives normal and pathological biological functions. In this paper we describe the biological, physical and mathematical concepts that led to the design of a Computational Morphogenesis (CM) platform baptized Generic Modeling and Simulating Platform (GMSP). Its role is to generate realistic 3D multi-scale biological tissues from virtual stem cells and the intended target applications include *in virtuo* studies of normal and abnormal tissue (re)generation as well as the development of complex diseases such as carcinogenesis. At all space-scales of interest, biological agents interact with each other via biochemical, bioelectrical, and mechanical fields that operate in concert during embryogenesis, growth and adult life. The spatio-temporal dependencies of these fields can be modeled by physics-based constitutive equations that we propose to examine in relation to the canonical biological events that occur during embryogenesis.

**This is Part 1 of a 2-part series that will cover the following. This paper (Part I) describes the core biological ontology underlying morphogenesis and the physics-based constitutive equations associated to the ontology. The second paper (Part II) will describe agency, system architecture and knowledge representation.

Keywords: biology of development, computational morphogenesis, computational biology, agents

1. Introduction

Basic and applied researches in the life sciences propose to unravel the mechanisms of life, support diagnosis and cure diseases. Much current information technology (IT) research applied to biomedicine is devoted to correlating molecular biomarkers with individual patient traits and diseases in order to advance towards personalized medicine. There is a widespread interest in processing "omics" data with artificial intelligence (AI) and data analytics technics (i.e. "Big Data"). These technics can map raw biological data into reduced forms such as regression models or probability density functions, and perform pattern-matching tasks using kernel-based methods such as Support Vector Machines or the increasingly popular "deep learning" approach. Although these technics are part of the personalized medicine tool-kit they fall short in terms of elucidating the actual mechanisms that underlie normal and pathological biological functions.

An in-depth understanding of the interdependencies between molecular, cellular, biomechanical and bioelectrical events and their roles in the development of tissue shapes and functions will open avenues for developing novel diagnostic and therapeutic tools. Theoretical and computational models have been designed to model mechanisms in biological systems long before the omics revolution began. However, their application in real-life problems has been relatively limited. Part of the explanation lies in the fact that modeling biological systems is a hard and lengthy process and the data necessary for model development and calibration is often missing. As a result, most modeling activity focuses on specific sub-topics such as gene regulatory networks, heart electrodynamics or first-order pharmacokinetics. Yet current results in molecular and cellular biology highlight the fact that cells' behavior depend on multi-modal local and global cues that span across multiple scales (Gilmour et al., 2017). The advances made by the growing field of tissue engineering in which cultures of 3D tissues and organoids are developed, support this view (Eyckmans and Chen, 2017; Takasato et al., 2015; Teague et al., 2016; Sachs et al., 2017) and a worthy goal for the computational biology community is to develop "dry-lab" frameworks that will provide a unifying view of living matter across all space-scales of interest and thus contribute in a concrete way to the efforts deployed by experimental and clinical research.

The framework specifications would describe how to represent and model the dynamic causal chains that operate from the genes to an organism's environment and from the latter back to the genes. In addition to contributing to a deeper holistic understanding of living organisms, such a platform would provide an environment for *in virtuo* experimentation that would serve as a support to hypothesis-formation and experimental design. The computing challenge then is to develop multi-scale models

that have both explanatory and predictive power; i.e. they should be complete enough to explain past and current available data, as well as predict plausible outcomes of new experimental protocols. The design of computational models of multifunctional realistic tissues could be a possible option that can be justified for a number of reasons. In living organisms there is a tight interdependency between biological functions and forms, e.g. an organ's shape (at least partly) explains its function and vice versa. Thus realistic modeling of living systems requires the embodiment of functions and forms. This constitutes a huge challenge since tissues have highly specialized, intertwined, fractal-like structural and functional organizations. Indeed, self-similar modules seem to characterize living matter. Any tissue region and any of its embedded sub-regions - down to small groups of individual cells - is always associated with at least the following: specialized cell-types organized into functional units, supporting cast of protective cells, sensory and control neurons, and the mass transport systems provided by the vascular and lymphatic networks.

Building realistic multi-scale computer models of living tissues is thus simply daunting and we argue that *only* a *generative* process has a real possibility to carry-out the task. That is, 3D models of mature tissues and organs should be computer-generated from pre-defined easy-to-model initial conditions involving stem cells embedded within a mesenchyme of simple geometry. One logical direction could be to develop the field of Computational Morphogenesis (CM) that would incorporate the self-organizing principles of embryogenesis. Developing CM could serve many purposes and not the least of which would be to assist stem cell technologies, organoid and tissue engineering as well as pharmacological and medical research. For instance, it has been postulated that complex diseases such as cancer are related to developmental processes insofar as carcinogenesis shares common features with normal embryogenesis (Höckel, 2015). In other words, cancer and complex systemic diseases could use the same conserved "tools" as the developing embryo, only at the wrong time and/or the wrong place. Thus, a closer look at the "toolbox" of embryonic development may help shape the modeling task in many life-science applications. Since ontogeny follows phylogeny, studying the underpinnings of embryogenesis, is also studying the conserved mechanisms underlying post-embryonic growth, adult tissue homeostasis and pathogenesis.

The main purpose of this paper (Part 1) and its sequel (Part2) is to examine in general terms what conceptual and computational tools can be drawn from biology, chemistry, physics and mathematics in order for CM to become a reality. Section 2 starts with biology and examines species-invariant molecular and cellular mechanisms that underlie all morphogenetic processes. These elementary mechanisms constitute the biological modules that underpin all morphogenetic events, and their conceptualization forms part of our core biology ontology (often written in italic). Section 3 describes current approaches in computational biology, and section 4 will detail the relationships between the core biological modules and their physical and mathematical underpinnings.

2. Basic events and mechanisms in developmental biology

2.1. The main phases of embryogenesis

In vertebrates, embryogenesis consists in studying the development of an embryo from the fertilized ovum (Wolpert et al., 2002). After the fertilization of the egg by a sperm, *cleavage* begins and consists of rapid mitotic divisions resulting in a spherical ball of 16 small cells called the *morula* that reorganizes into a *blastula* consisting of hollow sphere of cells surrounding an inner fluid-filled cavity (Wolpert et al., 2002). *Gastrulation* then follows in which cells commit to a specialized developmental path and form a three layered structure called the *gastrula* that is composed of the *mesoderm*, *endoderm*, and *ectoderm.* Each layer (also called germ-layer) constitutes a *domain* that will give rise to specific tissues and organs in the developing embryo (Wolpert et al., 2002; Tanaka, 2016; Vize et al., 2003). The ectoderm develops into both the epidermis and the nervous system. The mesoderm gives rise to muscle, cartilage, bone, and other internal organs like the heart, kidney, and connective tissue such as the blood, and the endoderm gives rise to the epithelium of digestive tract gut and lungs, as well as the liver and the pancreas (Wolpert et al., 2002; Tanaka, 2016). This process called *cell determination*, or alternatively *cell fate specification* comes under the influence of *morphogenetic fields* (Turing, 1952), and results in cells that are already partly *specified* by molecular *determinants* such as transcription factors. *Neurulation* and *organogenesis* follows gastrulation where the ectoderm, endoderm, and mesoderm develop into the internal organs and tissues of the organism. Embryonic development and morphogenesis are regulated by highly conserved genes (Tanaka, 2016; Lienkamp et al., 2012; Gilmour et al., 2017), gene products, as well as molecular and cellular mechanisms that carry over into adult life (Wolpert et al., 2002; Wang et al., 2014). In all phases of embryogenesis and in adult life, all cells exhibit a limited set of behaviors including *mitosis*, *cell fate determination*, *cell polarization*, *cell shape deformation*, *cell differentiation*, *cell-cell adhesion*, *cell-ECM adhesion, cell migration*, or *apoptosis*. The collective behavior of cells will in turn characterize tissue-level events that can also be described in terms of a limited set of basic biological processes. The set includes *cellular induction*, *lateral inhibition*, *cell condensation, tissue polarization, elongation, branching,* and *lumen formation.* A comprehensive analysis of these core concepts, at the molecular, cellular and tissue scales, is a necessary step towards implementing a generic CM platform.

2.2. Cellular Induction and lateral inhibition

In cellular induction (CI), morphogens secreted by one group of cells influence the behavior and/or fate of another neighboring group of cells (Wolpert et al., 2002; Vize et al., 2003). CI plays a key role in cell-fate specification and thus in organogenesis since morphogens activate transcription factors that control cell differentiation through the establishment of tissue-specific gene-expression profiles (Gilmour et al., 2017). As cells become increasingly specified, they get closer to their final differentiation identity and thus to their concluding functional roles (Wolpert et al., 2002). A cell(s response to a morphogen is closely correlated to its *identity* that, in turn ca be defined by expressed transcription factors. For instance, during nephrogenesis, mesenchyme cells that express the

transcription factor SIX, will not respond to the morphogen Wnt9 while SIX^- cells which are nephron progenitors will (Costantini and Kopan, 2010). CI can be broken down into *permissive* and *instructive* induction (Wolpert et al., 2002). In permissive induction, cells will produce only one kind of response to a signal when a given threshold is reached. In instructive induction, cells will respond differently to different concentrations of the signal. A well-known example of instructive induction is Wolpert's "French flag" in which cells will respond according to three distinct modes, "blue", "white" and "red", depending on their distance from the morphogen source. The inductive cells convey *positional information* by secreting morphogens that other cells sense (Wolpert et al., 2002; Vize et al., 2003). Hence positional information should be understood as a relative measure, not one with respect to a fixed coordinate system. An example of morphogen-based cell-fate specification is given by the antero-posterior axis *domain determination* established during neurulation (Wolpert et al., 2002). The primary morphogen involved is the Sonic Hedgehog (SHH) ligand that also plays a key role in the development of the digits, limbs and brain (Wolpert et al., 2002; Duboc and Logan, 2009). In Xenopus, cells exposed to high concentrations of SHH will form the posterior digits while cells more distant to the SHH source and exposed to lower concentrations will develop into the anterior digits (Duboc and Logan, 2009).

Induction is a generally reciprocal process involving distinct cell types or regions (fig. 1). Mutual induction can be observed between epithelium and mesenchyme during the organogenesis of secretory glands (Pan and Wright, 2011), lungs (Weaver et al., 2000) and kidneys (Vize et al., 2003; Costantini and Kopan, 2010) across many species. For instance, in the developing kidney, the metanephric mesenchyme (MM) induces ureteric bud (UB) growth and branching by secreting Glial Derived Neurotrophic Factors (GDNFs) and Fibroblast Growth Factors (FGFs). Concurrently, the UBs induce the MM via signals that include "wingless" Wnt9b signaling molecules which contribute to MM cell condensation and mesenchyme to epithelial (MET) transition (Costantini and Kopan, 2010; Krause et al., 2015). In a similar fashion, UB tip cells express Wnt11 that signals to the MM to upregulate GDNF. Induction requires both a signal and a signal receptor. In the kidney, reciprocal induction can only be actualized if UB tip cells express RET/FGFR receptors and the condensing mesenchyme cells express Wnt receptors (Vize et al., 2003; Costantini and Kopan, 2010). FGF receptors belong to the important class of Receptor Tyrosine Kinase (or RTK) family, and pathways activated by RTKs include the mitogen activated protein kinase (MAPK) pathway that plays a significant role in tissue growth and in diseases such as cancer (Wang et al., 2014). Wnt receptors belong to the *Frizzled* family of G-coupled proteins receptors (GCPR) that, with the RTKs, constitute two of the most important classes of membrane receptors involved in development and post-embryonic homeostasis (Weaver et al., 2000; Yu et al., 2009; Krause et al., 2015).

Like in all biological process, the control of CI is mediated by negative/inhibitory feedbacks. While positive feedbacks underlie self-sustaining or self-enhancing processes, negative feedbacks stabilize processes that must operate within physiological norms. For instance, the morphogenesis of the kidney collecting ducts is characterized by multiple iterations of reciprocal induction between the ureteric buds and the surrounding mesenchyme involving positive feedbacks mediated by GDNF/Ret and FGF/FGFR, and negative feedbacks mediated by the Bone Morphogenetic Proteins (BMPs) pathways (Vize et al., 2003; Costantini and Kopan, 2010; Krause et al., 2015; Nigam and Shah, 2009).

Like many other morphogens, the BMPs have also important functions in mature tissue homeostasis (Wang et al., 2014).

Inhibitory mechanisms such as *lateral inhibition* (LI) have a pattern-forming role (Wolpert et al., 2002; Pan and Wright, 2011; Weaver et al., 2000). In LI a cell that is committed to follow a developmental path can emit an inhibitory signal that will prevent neighboring cells to follow the same path (Wolpert et al., 2002). The role of LI has been studied in the periodic patterning of feathers and dots and stripes in the animal skin (Wolpert et al., 2002; Pan and Wright, 2011). LI is not limited to soluble morphogens however since it also prevails in direct cell-cell contact. For instance, the ubiquitous and conserved Delta/Notch pair is a membrane ligand-receptor system and has been studied in many developing organs such as the pancreas (Pan and Wright, 2011), the brain (Formosa-Jordan et al., 2013) and in branching morphogenesis in general (Varner and Nelson, 2014). In the developing pancreas, committed endocrine progenitors expressing membrane Delta ligand can prevent neighboring cells that express Notch receptors to acquire the same fate via this inhibitory signaling system (Pan and Wright, 2011). Also, recent studies show that the formation of extracellular gradients can involve species other that the morphogen itself (Yu et al., 2009; Wang et al., 2016). In what the authors call “restricted extracellular diffusion”, a morphogen such as FGF8 can react with other molecular species such as heparan sulfate proteoglycan (HSPG) that act as either inhibitors or facilitators to fine tune morphogen gradients (Yu et al., 2009).

2.3. Cell condensation

The *condensation* of mesenchymal cells results from their collective migration and aggregation in response to chemical, electrical and mechanical signals. Mesenchyme condensation is essential for recruiting the cells that will constitute the anlage of specialized functional units such as the kidney nephron (Vize et al., 2003; Urban et al., 2006; Costantini and Kopan, 2010), the breast mammary tree (Howard and Gusterson, 2000), and the limbs (Oberlender and Tuan, 1994; Frenz et al., 1989; Hall and Miyake, 2000). Various molecular and cellular mechanisms have been studied in order to explain cell condensation. They include upregulated N-cadherins expression reflecting increased cell-cell adhesion (Oberlender and Tuan, 1994), local differences in cell-ECM adhesion (Frenz et al., 1989), and local changes in cell proliferation (Hall and Miyake, 2000). Several studies have revealed that collective migration can result from antagonistic signals (Mammoto et al., 2011). In the developing tooth, mesenchyme cell condensation can result from antagonistic FGF8 and semaphorin morphogens (Mammoto et al., 2011). The FGF8 molecules secreted by the epithelium induce the mesenchymal cells to migrate towards the epithelial-mesenchymal interface by following the steepest FGF8 gradient (see also figs 1 & 2). However, near the interface, the mesenchymal cells are also repelled by a short-range repulsive semaphorin, Sema3f, thus creating a zone of cell compaction (Mammoto et al., 2011) that can also play a role in the determination of cell fate. Cell compaction results in smaller cell sizes that can modulate the cells’ sensitivity to differentiating chemical cues. Cell deformations lead to cytoskeletal changes that are transduced by mechanoreceptors and elicit specific cellular responses (Gilmour et al., 2017; McBeath et al., 2004).

2.4. Cell and tissue polarization

Cells are polarized when membrane domains or "poles" are structurally and functionally distinct from one another. All normal epithelial tissues have basolateral/apical axes that reflect functionally distinct domains. Cell polarization (CP) is necessary for cell migration, differentiation and the self-organizing collective behavior of cells during tissue segmentation (figs. 1-3). Following mesenchyme condensation, the coordinated assembly of cells that will give rise to epithelial structures such as epithelial trees is dependent on CP (Vize et al., 2003; Costantini and Kopan, 2010; Karner et al., 2009; Wang et al., 2017). Defects in this process have been associated to tissue disorganization and tumorigenesis (Macara and McCaffrey, 2013). The intracellular markers of cell polarization are polarity proteins that are differentially distributed between the poles (Axelrod and Bergmann, 2014). Much like induction and lateral inhibition occurring at the tissue level, CP is a *symmetry-breaking* event that is mediated by local positive and negative feedbacks (Axelrod and Bergmann, 2014). Epithelial cells exhibit apical, lateral and basal polarities that underlie coordinated tissue growth and shaping during morphogenesis (Gilmour et al., 2017; Karner et al., 2009). For instance, homotopic cell junctions occur between the lateral sides of epithelial cells while the formation of basal membranes will always develop at their basal poles. In post-embryonic life, cell polarity allows epithelial organs to carry-out their functions due to differences in the absorption and secretion of molecular species between the apical and the basal domains (Walck-Shannon and Hardin, 2014; Gilmour et al., 2017). Planar Cell Polarity (PCP) is another morphogenetic process in which cells can exhibit directional collective behavior within the epithelial plane. PCP plays an essential role in tissue-shaping insofar as coordinated cell deformations and spatial cell rearrangements use the epithelial plane as a directional cue (Gilmour et al., 2017, Karner et al., 2009; Axelrod and Bergmann, 2014; Walck-Shannon and Hardin, 2014). From a molecular perspective, the core PCP protein systems include the Frizzled/Flamingo system which is a component of the so-called non-canonical Wnt/PCP pathway (Maung and Jenny, 2011).

2.5. Tissue elongation

Tissue elongation is contemporaneous to tissue growth and is driven, among other mechanisms, by reciprocal cellular induction, lateral inhibition, and cell protrusions. There are at least two main events that drive tissue elongation: *oriented cell division* and *convergent extension*. In oriented cell division (OCD), cells either divide parallel or orthogonally to the plane (or wall) of the tissue layers (Ragkousi and Gibson, 2014). Tissue elongation such as epithelial tubule lengthening under the control of morphogen gradients involves parallel OCD (Vize et al., 2003; Costantini and Kopan, 2010). In this case, elongation is initiated by cell sorting and convergent migration (condensation) of pro-epithelial cells followed by the mutual induction between mesenchyme and the growing epithelial bud in which tip cells collectively migrate in the direction of morphogen gradients (Vize et al., 2003; Costantini and Kopan, 2010) (figs. 1-3). Cells divide parallel to the tubule wall, i.e., the mitotic spindles are oriented in the direction of the tubule main axis (Bergstralh et al., 2013), therefore post-mitotic cell growth induce cells further downstream to move forward leading to the lengthening of the tubule. In parallel OCD, cells usually divide symmetrically, thus under normal conditions the

daughter cells inherit the same cell fate as the mother cell (Bergstralh et al., 2013). In orthogonal OCD, the mitotic spindles of the dividing cell are orthogonal to the epithelium plane (or wall). The immediate surrounding of the daughter cell is distinct from that of the mother cell and may lead to asymmetric cell division with a development path that differs from that of the mother cell (Ragkousi and Gibson, 2014; Dewey et al., 2015). Tissue elongation can occur in the absence of mitotic activity by convergent extension (CE). In CE the tissue narrows in one direction (width) while extending in the orthogonal direction (length). This concerted directional behavior presupposes planar cell polarity (PCP). Intercalating cells will first protrude to create a wedge between adjacent cells in the direction that is perpendicular to the axis of elongation and generate so-called rosettes where the elongated and narrowed cell membrane domains meet at the center of the rosette. Elongation proceeds when rosettes resolve by intercalation (Karner et al., 2009; Walck-Shannon and Hardin, 2014). Studies have demonstrated that rosette-based CE participates in the elongation of kidney collecting duct tubules (Lienkamp et al., 2012).

2.6. Tissue folding and branching

Many organs feature the presence of a tubular architecture, usually consisting of a central lumen surrounded by single or stratified layers of epithelial cells. Tubular structures range from single tubes such as the intestine to complex branching patterns, as observed in the pancreas (Shih et al., 2013), the airways of the lungs (Weaver et al., 2000), the collecting ducts of the kidneys (Vize et al., 2003; Costantini and Kopan, 2010) and the mammary glands (Wang et al., 2017; Nigam and Shah, 2009). There are two geometrically distinct types of branching: budding and bifurcation also referred to as clefting. Budding corresponds to the formation of a new branch from an epithelium progenitor anlage or from the lateral side of a preexisting branch (Wang et al., 2017). Clefting splits a preexisting branch tip into several tips and can result from two main distinct processes: epithelial folding (Gilmour et al., 2017; Nerurkar et al., 2016; Savin et al., 2011; Bard and Ross, 1982; Tallinen et al., 2014) and matrix-driven branching (Varner and Nelson, 2014; Wang et al., 2017). Mechanisms that can explain epithelial sheet folding include concerted apical constriction (Gilmour et al., 2017; Varner and Nelson, 2014), differential growth between adjacent tissues (Bard and Ross, 1982) and mechanical buckling (Varner and Nelson, 2014; Nerurkar et al., 2016; Savin et al., 2011; Tallinen et al., 2014). Apical constriction (AC) requires the coordinated constriction of the epithelial cells' apical domains with planar cell polarity (PCP) being a coordinating factor (Gilmour et al., 2017, Varner and Nelson, 2014). It was first observed during the neurulation phase of the chicken embryo in which the neuro-epithelial ectoderm folds to form the neural tube (Jacobson and Gordon, 1976; Wolpert et al., 2002). Concerted AC is the cause of the clefting observed in the developing kidneys, lung and pancreas and can be initiated by morphogens (Gilmour et al., 2017; Wang et al., 2017). The concerted apical constrictions create a difference in the radius of curvature between the basal and apical domains of the epithelial sheet leading to an invagination of the epithelial tissue. At the molecular level, AC requires apical recruitment of regulators of cell-contraction such as the ubiquitous Rho/ROCK system (Gilmour et al., 2017; Nishimura and Takeichi, 2008). Rho/ROCK complexes modulate the contraction of the actin-myosin fiber networks present at the apical cell domain. The expression of Rho/ROCK is under the control of transcription factors that, in turn, can be regulated by paracrine morphogens secreted by neighboring cells such as GDNF for the kidney (Krause et al., 2015) or FGF for the lung (Wang et al., 2017). The second mechanism underlying epithelial sheet folding is differential growth between an epithelial sheet and a connected adjacent

tissue. Differential growth corresponds to an increased number of epithelial cell divisions relative to the proliferation rate of the adjacent tissue resulting in a tangential growth differential. The faster growing tissue develops against the constraints of the slower expanding one resulting in mechanical buckling. This mechanism has been observed during the morphogenesis of the gut (Nerurkar et al., 2016; Savin et al., 2011), the eye (Bard and Ross, 1982), and the brain (Tallinen et al., 2014). In the third, matrix-driven branching mechanism, a cleft is first initiated in the form of a gap between adjacent epithelial cells (Wang et al., 2017). Studies of the salivary glands show that branching is initiated by the formation of shallow clefts, which then deepen over time as a result of fibronectin accumulation at the site of the cleft in the epithelium (Wang et al., 2017). During the development of the pancreas, yet other studies have showed that branching is initiated via ECM-integrin signaling that regulates the tip cells adhesion and is concomitant to epithelial invagination rather than cleft formation (Shih et al., 2016). Fig. 4 illustrates a simplified version of branching.

2.7. Lumen formation

The formation of lumens is a central feature observed in many developing organs. All secreting glands and organs such as the lungs and kidneys feature the presence of tubular structures consisting of a central lumen surrounded by an epithelium. Other structures found in secreting glands are the acini that are spheroid-shaped epithelium surrounding a liquid-filled lumen. There are three main mechanisms that lead to the generation of lumen: the formation of cavities (or cavitation) driven by cell death (Macias and Hinck, 2012; Debnath et al., 2002), epithelial sheet separation underlined by cell polarity (Martín-Belmonte et al., 2008; Pearson et al., 2009; Strilic et al., 2010), driven by fluid lumen inflow (Pearson et al., 2009), and/or cell-cell repulsion due to electrostatic apical repulsion (Strilic et al., 2010). For tubule-forming processes, other mechanisms such as cellular remodeling have also been identified as lumen-forming mechanisms during mammary duct growth (Macias and Hinck, 2012; Ewald et al., 2008). In cavitation, the lumens are formed from spheroids of compacted cells (cellular condensation) in which cells located in the interior of the spheroid undergo apoptosis (Debnath et al., 2002) and/or autophagy (Macias and Hinck, 2012; Debnath et al., 2002). Cells in contact with the ECM adopt polarized epithelial phenotypes while interior cells remain in less differentiated states and die. The second mechanism, membrane separation due to osmosis, is a fluid-filling process in which differences in osmotic pressure between the lumen and the mesenchyme and stroma result in asymmetric fluid movement towards the cavity (Pearson et al., 2009; Navis and Nelson, 2016). One of the fluid-filling processes is driven by ATP dependent Na+/K+ pumps that drive ion -and therefore- fluid movement between the epithelial cells' basal and apical domains leading to the formation of an open luminal space (Pearson et al., 2009). The third mechanism involves electric fields that can initiate lumen formation in endothelial chords due to cell-cell repulsion of polarized endothelial cells carrying negatively charged proteoglycans at their apical domain (Strilic et al., 2010). Once lumens are formed, they can expand by the subsequent addition of epithelial cells that result from oriented cell division and/or cell intercalation. The control of lumen size can be established by processes such as proliferative suppression (Debnath et al., 2002). Both lumen formation processes involve cell polarization, the formation of cell-cell junctions, and cell-ECM interactions (Martín-Belmonte et al., 2008; Hebner et al., 2008); and disruption of these processes can lead to carcinogenesis (Hebner et al., 2008). Although multiple mechanisms underlie tissue branching, elongation and lumen formation, they all derive from coordinated base molecular and

cellular events. The latter include cell sorting and condensation, cell polarization, cell fate determination and differentiation, PCP, patterned cell proliferation such as OCD, coordinated cell deformation, and cell rearrangement due to short and long migratory processes. These are morphogenetic "modules" that mirror conserved patterns of molecular signaling pathways that feature positive and negative feedback loops within the cells, across adjacent cells and over multiple cells. These multi-scale feedback loops are responsible for the symmetry-breaking events observed at the molecular (e.g. PP asymmetry), cellular (e.g. cell polarity) and tissue level (e.g. branching).

2.8. Morphogenetic electric fields

While the literature on the chemical and the mechanical cues of morphogenesis is quite extensive, much less attention seems to have been devoted to the role of electromagnetic fields in intercellular communication. Like their molecular and mechanical counterparts, electric fields (EF) have an effect on gene-regulatory networks that control cell proliferation (Lang et al., 2005), migration (Funk, 2015), and differentiation (Adams and Levin, 2013). Experimental results show that most cells can robustly orient polarity, migration, or division with respect to applied EF of magnitudes similar to those measured *in vivo* (Gao et al., 2011). Thus EF-induced cell behavior corroborates the role that EFs play in morphogenesis. EFs are involved in patterning and symmetry-breaking in the early embryo; e.g., antero/posterior or left/right patterning (Adams et al. 2006; Adams and Levin, 2013; Beane et al., 2013), in cell polarization (Adams and Levin, 2013), cell shaping (Pan and Wright, 2011), and lumen formation (Strilic et al., 2010). In the development of post-ganglionic neurons, neurites retract in the direction perpendicular to the electric field but grow the direction parallel to it (Pan and Wright, 2011). Regarding migration in general, EF can override other cues (e.g. chemical, topographic cues) in which, for instance, the direction of electrotaxis may differ from that of chemotaxis (Funk, 2015; Gao et al., 2011). Interestingly, EF patterns can precede and predict major morphological events such as the point of emergence of the limb bud in the amphibian embryo (Funk, 2015). EF and electrical currents are also associated with large-scale tissue behavior such as wound healing and directional migration of epithelial cells into the wound bed (Funk, 2015). In the nervous system, tissue regeneration studies have shown that EFs induce the directed growth of nerves of the spinal cord (Funk, 2015). More generally, it has been demonstrated that the central nervous system and neurotransmitters are implicated in the morphogenetic processes of tissue regeneration (Durant et al., 2015). In view of these biological facts, cellular electrodynamics must be fully integrated within CM platforms.

3. Current modeling approaches of morphogenesis and beyond

3.1. Continuum models

Continuum models represent tissues as macroscopic continuous materials and are solved by partial differential equations (PDE) or integro-differential equations (Cristini et al., 2009; Lowengrub et al., 2010). Most continuum models in embryology are reaction-diffusion (RD) systems based on the

seminal work of Alan Turing (Turing, 1952). Application of RD systems include patterning on animal skin (Yamaguchi and Yoshimoto, 2007; Hiscock and Megason, 2015), tissue growth and branching (Menshykau et al., 2014; Iber et al., 2015), limb formation (Dillon and Hans, 1999), and cell migration and cell sorting (Painter, 2009). Continuum models have also been applied to study the biomechanics of morphogenesis (Dillon and Hans, 1999; Munoz et al., 2010; Shi et al., 2014) as well as cancer growth (Macklin and Lowengrub, 2008). In recent cancer models, continuum models have been extended to include the migration of cells wherein individual cells are replaced by cell volume fractions (Cristini et al., 2009; Lowengrub et al., 2010). One of the drawbacks of continuum models stems from the fact that cells are represented as passive entities -like chemical substrates- subject to "forces" derived from the gradients of intercellular chemical fields with no real autonomy of their own. Non-linear behavior resulting from small changes in the cells' environment cannot easily be modeled with continuum models, no more than the complex decision-making that cells need to perform in the presence of multi-modal external cues. In all situations, cells respond to external stimuli by adopting discrete and modulated behaviors as has been described in section 2. Another drawback of continuum models is that their solutions may be unstable and yield tissue contours of low fractal dimensions whereas real tissues can exhibit sharp edges due to tissue discontinuities and cell heterogeneities.

3.2. Discrete models

All discrete models share the common view that the world has a granular nature. Formalisms based on discrete objects include graph theory (Meyers et al., 2005), boolean networks (BN) (Saez-Rodriguez et al., 2009), petri nets (Chaouiya, 2007), cellular automata (CA) and variants (Siregar et al., 1998; Piotrowska et al., 2009; Torquato, 2011; Chen and Torquato, 2014; Gunji and Ono, 2012). Other discrete models include Cellular Potts Model (CPM) (Graner and Glazier, 1992; Glazier and Graner, 1993; Li and Lowengrub, 2014), Particle based models (Honda et al., 2000; Meineke et al., 2001), and stochastic cell population dynamics (Chmielecki et al., 2011; Bauer et al., 2015; Gupta et al., 2009). Boolean networks and Petri nets are widely used to study intracellular networks (Saez-Rodriguez et al., 2009; Chaouiya, 2007) while a CA is universal machine composed of identical cells that can take one of a finite number of state. In CA, cells evolve in parallel and at discrete time steps following state transition rules where each cell's transition will depend on the states of its neighbor cells only (Wolfram, 2002). CAs can cover topics as different as the heart electrical activity (Siregar et al., 1998) and tumor growth (Piotrowska et al., 2009; Torquato, 2011; Chen and Torquato, 2014). CPM mimic the differential adhesion of cells as the main cause of tissue-patterning and in which cells of the same kind will more likely adhere (lower adhesion energy) than cells of different types. CPM draw their formalism from the Ising model and phase transition phenomena in ferromagnetic materials and use Monte Carlo technics to compute cell displacement (Graner and Glazier, 1992). In lattice-free particle-based models, cells or aggregates thereof are represented by soft spheres where collective behavior is defined by inter-particle interaction rules. Particle-based spheroid models of cells have been used to study pattern formations in the butterfly epidermis (Honda et al., 2000) and the intestinal crypts (Meineke et al., 2001). Finally, stochastic population dynamics have applications in many fields, notably to study cancer initiation and growth (Bauer et al., 2015), cancer treatment (Chmielecki et al., 2011) and cancer cell heterogeneity (Gupta et al., 2009). Discrete deterministic

and stochastic models are very informative in assessing *emerging* properties from simple local rules or interactions. However, the rules are often purely phenomenological and are not concern with mechanistic explanations. In addition, barring few exceptions (e.g. Bandini and Mauri, 1999; Dascalu et al., 2011; Portegys et al., 2016) most rule-based system also account for local interactions only and are thus not suited to study medium and long range interactions. This issue has been addressed in nested rule-based models wherein "nested neighborhoods provide a straightforward representation of a morphogenetic field that contains a hierarchy of local vs. global information" (Portegys et al., 2016). To the best of our knowledge however, rule-based systems are mostly 2D systems that seem to lack the mechanistic finess to address the simultaneous and reciprocal top-down and bottom-up multi-modal interactions that hold between macroscopic systems (e.g. tissues) and microscopic agents (e.g. cells or genes). As in all dynamic systems, time plays a critical role in biological systems, and CA-type models experience difficulties in capturing all at once, slow and transient extracellular advection/diffusion processes with distinct space-time characteristics, fast and transient action potentials, and even much faster volume-conducted electrical and magnetic fields.

3.3. Hybrid models

Hybrid models (HM) combine features of both continuum and discrete methods. At the mesoscopic scale, cells and tissues can be represented as discrete entities while chemical species are represented as continuous fields. HM typically combine continuum reaction-diffusion equations with cells represented as discrete entities and responding to chemical cues in the micro-environment (Gevertz and Torquato, 2006; Anderson et al., 2006), or chemical and mechanical cues (Kim and Othmer, 2013). Cells can be represented as particle-like objects with soft sphere interaction potentials or as polygons in more detailed vertex-based models (VBM). In VBM, each pair of neighboring cells is represented by a common edge and the points of intersection by vertices. VBMs have been used to study the mechanical aspects of cells and tissues, notably during morphogenesis (Fletcher et al., 2014). Another type of hybrid model is the 2D IBCell in which cells are approximated by polygons (Rejniak, 2007; Rejniak et al., 2007). In contrast to the VBM cells, 2D IBCell cells do not share edges. 2D IBCell edges represent real cell membrane defined by a set of massless points that are advected by fluid flow. A hybrid multi-scale framework in 2D is MecaGen (Delile et al., 2017). Like other multi-scale approaches (e.g. (Kim and Othmer, 2013)), MecaGen implements subcellular, cell-level and tissue level features. MecaGen includes paracrine ligand secretion and diffusion, signal transduction and gene switching along with cell mechanical responses.

3.4. Our proposition

Building computational models is a complex task, therefore most modeling efforts center on a main question to which they provide at least plausible answers. As a result, most models are built around one main modality: biochemical (Yamaguchi and Yoshimoto, 2007; Dillon and Hans, 1999; Gevertz and Torquato, 2006; Anderson et al., 2006; Kim and Othmer, 2013); mechanical (Beloussov, 2012; Varner and Taber, 2012; Munoz et al., 2010; Shi et al., 2014; Macklin and Lowengrub, 2008; Li and Lowengrub, 2014; Fletcher et al., 2014; Rejniak, 2007; Rejniak et al., 2007); electrical (Siregar et al., 1998; Law and Levin, 2015). From the point of view of (normal and abnormal) morphogenesis, most

models are focused around specific aspects: tissue growth (Cristini et al., 2009; Lowengrub et al., 2010; Piotrowska et al., 2009; Torquato, 2011; Chen and Torquato, 2014; Li and Lowengrub, 2014; Chmielecki et al., 2011; Anderson et al., 2006; Kim and Othmer, 2013; Fletcher et al., 2014; Rejniak, 2007; Rejniak et al., 2007; Delile et al., 2017); cell sorting and tissue segmentation (Painter, 2009; Graner and Glazier, 1992; Glazier and Graner, 1993); regular and periodic pattern formation (Yamaguchi and Yoshimoto, 2007; Hiscock and Megason, 2015; Dillon and Hans, 1999); elongation and branching (Menshykau et al., 2014; Iber et al., 2015; Gevertz and Torquato, 2006), tissue deformation and shaping (Munoz et al., 2010; Macklin and Lowengrub, 2008), chemo-mechanical early embryo morphogenesis (Delile et al., 2017). All address particular stages of development, e.g. early embryogenesis (Delile et al., 2017), as opposed to late embryogenesis wherein the morphogenetic role of blood circulation and CNS electrical activity must be accounted for. To the best of our knowledge, no current model addresses the critical role of bioelectric signals in morphogenesis to the exception of (Law and Levin, 2015; Levin, M., 2012). In terms of space scales, many models address one scale only: intracellular networks (Saez-Rodriguez et al., 2009; Chaouiya, 2007), the microscopic (e.g Piotrowska et al., 2009) or the mesoscopic scales (e.g. Cristini et al., 2009). As for population dynamics models they are not intended to address the spatial dimension and thus do not instruct on the primary role of the spatial dimension (local specificity). Finally, *in vitro* experimental data on tissue dynamics show that results in 2D differ from those obtained in 3D, yet the vast majority of models are limited to 2D e.g. and existing 3D models are, like their lower-dimension counterparts, focused on specific modalities and/or development stages. From a methodological standpoint, many models adopt either a deterministic or a stochastic approach and are based on computational technics such as cellular automata, petri nets, ODEs, PDEs, or optimal control (De Pillis and Radunskaya, 2001). Although there are good justifications for using a particular method, a number of works do acknowledge the advantages of combining continuum (PDE, ODE) with discrete methods, e.g. (Gevertz and Torquato, 2006; Delile et al., 2017). Other works see the advantage of combining mesh-free and grid-based formulations, e.g., (Rejniak et al., 2007). Still others incorporate deterministic and stochastic elements e.g. (Graner and Glazier, 1992; Glazier and Graner, 1993). The question that we are attempting to answer is the following: is it possible to build a generic CM platform dedicated to the generation of *structurally* and *functionally* realistic, hierarchical and modular 3D tissues that could include epithelia, parenchyma, stroma, CNS components, blood and lymphatic vessels and as well as immune cells? Only then, can such artefacts be invaluable for experimentalists because they will share, with experimentalists, the same representations of the biological world and thus "speak" the same language. It is much too early to answer this question but general comments can be made as follows. Modeling complex systems is a multistage process that starts from coarse-grained drafts and evolves towards more exact models following an incremental refinement loop. Multi-stage model refinement requires the ability of human and artificial agents to reason qualitatively (Siregar et al. 1995), causally (Siregar et al., 1993, Siregar and Toulouse, 1995), spatio-temporally (Siregar and Sinteff, 1996b; Siregar et al., 1997), bridge qualitative reasoning with semi-quantitative and quantitative data (Siregar, 1996a; Siregar et al., 1996c) and develop general computational tools (Siregar, 2000; Siregar et al., 2003) as well as AI-based agents specialized in specific areas such as model selection and model calibration (Siregar, 2009). Thus general and complementary tasks can be identified: (a) establish an ontology that explicitly defines the type of agents (e.g. cell lineage) that need to be modelled, what are their properties, and how they interact with each other; (b) identify and implement constitutive equations

that will model their interactions; (c) design a knowledge based system (KBS) that will incorporate all the data necessary to model the agents and to assist in the modeling task. Section 2 gave an introduction of task (a), and the ensuing discussion will address task (b). Deeper issues concerning ontologies and KBS design in morphogenesis will be discussed in the sequel (Part II) paper of this special issue.

4. The constitutive equations and their relation with morphogenesis

4.1. Chemical fields

The GMSP was initially designed to generate models of complex systems, open to their external environments (Prigogine, 1979), that would possess a hierarchical and modular architecture and the capacity to self-organize via the coordinated actions of multiple agents interacting across short, medium and large distances (fig. 5). During morphogenesis, the most studied and perhaps best known intercellular communication means is molecular signaling. It is believed that most morphogenetic processes depend, among other factors, on the formation of concentration gradients that can be established by different mechanisms that include the diffusion of soluble morphogens and the passing of signaling molecules across gap junctions. Cell fate can be determined by the presence of morphogens that can play the role of permissive and instructive induction agents. In both cases, the concentration gradients the will determine a cell's fate and this simple mechanisms has been shown to play a role in in tissue segmentation such as anterior/posterior patterning during neurulation (sect. 2.1, sect.2.2). Mutual induction between groups of cells can also rely on the concentration gradients of diffusing morphogens. When molecular concentrations are modeled as continuous scalar fields, their space-time dependencies can be modeled by the following constitutive equation

$$\frac{\partial u_i}{\partial t} = \nabla.(D_i \nabla u_i) - \delta_i u_i + s_i \qquad i = 1, \ldots, n \tag{1}$$

where u_i are the n chemical species concentrations, δ_i the decay rate, s_i the source terms, and D_i the diffusion tensors. The decay term $\delta_i u_i$ constitutes a "sink" and cover distinct and non-exclusive realities: molecular degradation, molecular adsorption (e.g. ligand-receptor binding), and molecular sequestration (e.g. pinocytosis). The source terms s_i correspond to high concentration regions that result from cells secreting the i^{th} molecular species. Examples of diffusing molecular morphogens include the Sonic Hedgehog (SHH) ligand that plays a key role in the development of the digits, limbs and brain (sect.2.2); and the FGFs, TGF-β and BMPs that induce chemotaxis during cell condensation in developing organs (sect.2.3). Processes such as oriented cell division are also under the control of inductive diffusing signals during tissue elongation (sect.2.5). In chemotaxis and oriented cell division, cells migrate (resp. divide) in the direction of the concentrations gradients ∇u_i .

Tissues and cells are, among other things, biochemical reactors in which reactants, intermediate molecular species and final products interact and diffuse. Intracellular metabolic networks (e.g. Krebs Cycle), transcription and gene regulatory networks are examples of coupled biochemical reactions.

The process of reacting agents that are transported by diffusion can be modeled by reaction-diffusion (RD) equations with sources and sinks:

$$\frac{\partial u_i}{\partial t} = f_i(\delta_i; u_1, \ldots, u_n) + \nabla.(D_i \nabla u_i) + s_i \qquad i = 1, \ldots, n \qquad (2)$$

where f_i represent the reaction terms. During morphogenesis, RD equations (rather than pure diffusion) can be applied to model "restricted extracellular diffusion" in which molecular species interact with the morphogen to fine-tune the morphogenetic gradients (sect.2.2) and a special case of RD equations have been developed to study short-range local enhancement as well as long-range lateral inhibition (sect. 4.3). RD processes are one of the hallmarks of morphogenesis (Gilmour et al., 2017).

Many models of sub-cellular level biochemical networks adopt the so-called "well stirred" assumption in which the diffusion terms can be ignored. Equation (2) becomes a system of ODEs representing purely reactive entities with time-varying concentration profiles.

$$\frac{du_i}{dt} = f_i(\delta_i; u_1, \ldots, u_n) \qquad i = 1, \ldots, n \qquad (3)$$

Intracellular network models in systems biology use this type of equation to study interactions among various molecular species involved in transduction, transcription, metabolic networks and host immune response (Eisenhammer et al., 1991; Wittmann et al., 2009) as well as predicting treatment outcomes (Peng et al., 2016).

At the latter stages of embryonic life and in the developed organism, long-range interactions (e.g. via hormones) and mass transport between organs are carried-out by the circulatory system. If we assume that blood is an incompressible isothermal fluid, the velocity profile of the flow is given, in the Eulerian view, by the Navier-Stokes equations (Zienkiewicz, 2005):

$$\rho\left(\frac{\partial \mathbf{v}}{\partial t} + \mathbf{v}.\nabla\mathbf{v}\right) = -\nabla p + \mu\nabla^2\mathbf{v} + \mathbf{f}_{ext} \quad (momentum\ equation) \qquad (4.1)$$

$$\nabla.(\rho\mathbf{v}) = 0 \qquad (continuity\ equation) \qquad (4.2)$$

where $\mathbf{v}$ is the fluid velocity, ρ is the density of the fluid, p is the pressure, μ is the dynamic viscosity of the fluid. Equation (4.1) describes the conservation of momentum and is basically Newton's 2nd law for a fluid while (eq. 4.2) expresses the conservation of mass. The left-hand side of the equation expresses the rate of change of momentum per unit volume and the right-hand side depicts the forces per unit volume (or force densities) involved in the momentum density rate of

change. In fluids, the force densities are the pressure-gradient (first term), viscous forces due to shear stress (second term), and external forces summarized in $\mathbf{f}_{ext}$ acting upon the local fluid element (e.g. gravity). Solving the Navier-Stokes equations are part of hybrid models such as the immersed boundary (IB) methods that have been applied to study tissue growth as well as the formation of tumors (e.g. Rejniak et al., 2007). During embryogenesis, once the circulatory system is in place, the molecular secretions in interstitial space and the transport from tissue to circulation and back to tissues is performed by advection and diffusion processes. The constitutive equation for advection-diffusion (with source terms) combines (eq. 1) and (eq. 4) and is given by:

$$\frac{\partial u_i}{\partial t} = \nabla.(D_i \nabla u_i) - \delta u_i + s_i + \nabla.(u_i \mathbf{v}) \qquad i = 1, \ldots, n \qquad (5)$$

where $\nabla.(u_i \mathbf{v})$ is the advection term and $\mathbf{v}$ is the local fluid velocity given by the Navier-stokes equations (eqs. 4). In the large vessels advection dominates (e.g. aortic flow), in the semi-permeable capillaries both advection and diffusion occur, and in the interstitial spaces, diffusion prevails (eq. 1).

Certain biochemical reactions occur in all vessels including large ones where advection is important. Hemostasis which prevents blood loss from damaged vessels via a coagulation cascade is an example (Versteeg et al., 2013). Damaged endothelium exposes the underlying collagen and Von Willebrands factors to which circulating platelets bind. This triggers a coagulation cascade that results in production of fibrin and the formation of a blood clot. The master equation describing the molecular component of such processes combines (eq. 2) and (eq. 4) that results in a reaction, diffusion, and advection (RDA) equation:

$$\frac{\partial u_i}{\partial t} = f_i(\delta_i; u_1, \ldots, u_n) + \nabla.(D_i \nabla u_i) + \nabla.(u_i \mathbf{v}) \qquad i = 1, \ldots, n \qquad (6)$$

Once the circulatory system is in place, some of development and growth processes that proceed via long-range interactions use the circulatory system as a chemical reactor.

4.2. Turing patterns

Allan Turing in seminal work on “The chemical basis of morphogenesis” (Turing, 1952) showed that ordered patterns such as stripes or spots observed in animals arise from the amplification of unstable fluctuations in an initially spatially homogeneous distribution of morphogens. This chemical instability known as “Turing instability” is induced by the diffusion term and must involve an activator and an inhibitor. As we have seen in (sect.2.2-sect.2.6) all biological functions are self-limiting, either directly or indirectly. Indirect inhibition takes place in negative feedbacks in which an inhibitor suppresses the agent that is responsible for its activation. Gierer and Meinhardt reformulated the general idea of Turing by proposing that all periodic or quasi periodic patterns could be modeled by local self-enhancement and long range inhibition (LELI) (Gierer and Meinhardt, 1972). Local self-enhancement is formulated as an autocatalytic process while long-range inhibition performs an

indirect self-regulatory role that ranges over a large distance. Gierer and Meinhardt studied a two-species RD system (eq. 2):

$$\frac{\partial u}{\partial t} = \frac{\rho u^2 + \rho_u}{v} - \delta_u u + \nabla.(D_u \nabla u) \qquad (7.1)$$

$$\frac{\partial v}{\partial t} = \rho u^2 - \delta_v v + \nabla.(D_v \nabla v) \qquad (7.2)$$

where u is the activator; v the inhibitor; ρu^2 the non-linear autocatalytic term; ρ_u is a low level activator quantity that initiates autocatalysis; $1/v$ the inhibitory term; ρ a competency factor, and d_u, d_v are decay rates. Stable patterning prevails if the diffusion coefficients and the partial derivatives of the reaction terms satisfy a number of conditions, notably that only if the activator diffuses more slowly than a longer range inhibitor (Turing, 1952; Gierer and Meinhardt, 1972; Gierer, 1981). This general patterning principle can be acknowledged in local positive feedback and lateral inhibition that arise within the cell during polarization (sect. 2.4), across multiple cells during budding and elongation (sect. 2.5), and during branching where a new branch can inhibit surrounding cells to also branch (sect. 2.6). Recent data obtained from different animal models support this general principle (Meinhardt, 2008; Kondo and Miura, 2010). However, Turing patterning solely based on coupled RD equations are known to be unstable and sensitive to initial conditions. Recent studies have shown that by incorporating biological factors such as tissue-specific expressions of ligand and receptor, robustness of the Turing mechanism can be obtained (Menshykau et al., 2014).

4.3. Electric fields

All cells and tissues are surrounded by electrical signals. Cells have transmembrane potentials that are maintained by cell membrane ATP-dependent ion pumps that drive ion species such as Na^+ and K^+ across the cell membranes and against transmembrane ion concentration gradients (Hodgkin and Huxley, 1952). These ion currents and the non-conductive and capacitive properties of plasma membranes create a potential difference between the cells' interior and exterior. Within the bidomain theory (Henriquez, 1993), relations between intra-cellular potentials ϕ_i, extracellular potentials ϕ_e with net transmembrane currents I_m, can be expressed by a couple of the steady-state diffusion equations which are derived from Ohms law and the principle of charge conservation:

$$-\alpha I_m = \nabla.(G_e \nabla \phi_e) \qquad (8.2)$$

$$\alpha I_m = \nabla.(G_i \nabla \phi_i) \qquad (8.1)$$

where G_i and G_e are, respectively the intra-cellular and extra-cellular conductivity tensors; α a scale factor corresponding to the cell surface to volume ratio; and I_m is the source term representing the net transmembrane current entering and leaving the cell. Using equivalent network theory for cell membranes (Hodgkin and Huxley, 1952; Catterall et al., 2012), the transmembrane current is defined as the sum of a capacitive term and a ionic term.

$$I_m = C_m \frac{\partial V_m}{\partial t} + I_{ion} \quad (9.1)$$

$$I_{ion} = \sum_i I_i \quad (9.2)$$

where C_m is the capacitance per unit area, V_m is the transmembrane potential, and I_i the contribution of the ith ion species to the transmembrane current. In living tissues, the main ion species include Na^+, Cl^-, K^+, Ca^{2+}, and Mg^{2+}. The source term I_m can be computed by Hodgkin-Huxley type (HH-type) equations named after the seminal work of Hodgkin and Huxley on the giant squid axon (Hodgkin and Huxley, 1952). Hodgkin & Huxley assumed that the ionic currents I_i obey Ohm's law,

$$I_i = g_i(V_m, t)(V_m - E_i) \quad (9.3)$$

where g_i is the macroscopic membrane conductance, $V_m = \phi_i - \phi_e$, and E_i the resting Nernst potential for the ith ion species. The time and voltage-dependent g_i is assumed to be generated by a large number of microscopic membrane channels. Two states (permissive, non-permissive) ionic gates regulate these channels. A channel is said to be open if all gates are in the permissive state and closed otherwise. Writing inward and outward currents' associated Nernst potentials by E_i and E_i' respectively, an HH-type equation has a general form that further specifies eqs. 9.1-9.3:

$$I_m = C_m \frac{\partial V_m}{\partial t} + \sum_i g_i(V_m - E_i) + \sum_k g_k'(V_m - E_k') \quad (10.1)$$

$$\frac{dg_i}{dt} = f_i\left(g_i; \alpha_i(V_m), \beta_i(V_m)\right) \quad (10.2)$$

$$\frac{dg_k'}{dt} = f_k\left(g_k'; \alpha_k(V_m), \beta_k(V_m)\right) \quad (10.3)$$

where α_j and β_j are the gate's voltage dependent rate constants for transitions between states. These equations and their subsequent variants have been developed to describe *excitable* cells such as neurons, myocytes, and muscle fibers (Hodgkin and Huxley, 1952; Catterall et al., 2012; Ten Tusscher et al., 2004; Noble, 1962; DiFrancesco and Noble, 1985). However, membrane potentials are observed in all cells and across epithelial sheets and in fact could be part of the cells' memory apparatus (Law and Levin, 2015). Slow changes in the resting plasma membrane potentials driven by ion channels, pumps and gap junctions serve as a highly conserved pathway that regulates cell

proliferation, migration, differentiation and apoptosis (Levin, 2014; Lang et al., 2005). Long-range electrical coupling is realized by a network of gap junction channels between neighboring cells, and through them, membrane potentials act as regulators of pattern formation in embryogenesis and their variations. Membrane potentials have also been shown to induce non-mutated cells to adopt cancer cell phenotypes (Chernet and Levin, 2013) and recent cancer studies have shown that the spatial distribution of an external biochemical agent can modify the conductances of the ion channels in a cell membrane and thus the cell membrane potential V_m (Fraser et al., 2014) leading to possible therapeutic targets (Arcangeli et al., 2009). From a modeling standpoint, variations in the electrodynamics of cells can be studied by exploring how a chemical species can impact the gating functions, g_i, and their rate constants α_j and β_j (eqs. 10.2, 10.3).

Once the current-source I_m has been computed, the extra-cellular electric fields can be predicted from (eqs. 8 and 9) by redefining the intra-cellular potential ϕ_i in terms of V_m and the extra-cellular potential ϕ_e. This yields a set of two coupled equations: a reaction-diffusion equation,

$$\frac{\partial V_m}{\partial t} = \frac{1}{\alpha C_m}\left[\nabla.\left(G_i \nabla\left(V_m + \phi_e\right) - \alpha I_{ion}\right)\right] \qquad (11)$$

and an implicit elliptic equation

$$\nabla.\left(\left(G_i + G_e\right)\nabla\phi_e\right) = -\nabla.\left(G_i \nabla V_m\right) \qquad (12.1)$$

$$G_e \nabla\phi.\mathbf{n} = 0 \qquad (12.2)$$

where ϕ_e satisfies the no-flux von-Neumann boundary condition (i.e. skin):

The extracellular potential ϕ_e, can be obtained by solving the elliptic eq. 12, and from ϕ_e the extracellular electric field (EF) can be derived:

$$\mathbf{E} = -\nabla\phi_e \qquad (13)$$

The analysis and simulation of volume conducted bioelectric potentials and EF are carried-out in many fields including electrocardiography (Siregar, 1996a; Siregar et al., 1998; Henriquez, 1993; Pezzuto et al., 2017), electromyography (Fernandez et al., 2016) and electroencephalograpy (Siregar et al., 1989; Lopez Rincon and Shimoda, 2016). Theoretical and computational results obtained from these fields can be exported to CM. The bidomain theory and its monodomain simplifications applies to any tissue since cells are the microscopic generator of the measured macroscopic extracellular potentials. As discussed in sect.2.8, bioelectrical signals contribute in all the phases of embryogenesis as well as in wound healing and tissue regeneration and in which neurons of the CNS are involved (Funk, 2015). They also play a role in disease initiation and evolution. Defects in ion transport and the correlative changes in transmembrane potentials V_m, volume conducted electric fields $\mathbf{E}$, and

electrical signaling via gap junctions have been associated with diseases such as cancer (Chernet and Levin, 2013; Fraser et al., 2014), kidney, or heart diseases (Ten Tusscher et al., 2004).

4.4. Mechanical fields

Biomechanics is involved in all morphogenetic processes as it underlies cell motility, cell adhesion and cell deformation, and global morphogenetic processes such as branching (sect.2.6), buckling (Beloussov, 2012; Varner and Taber, 2012), convergent extension (Varner and Taber, 2012) and biomechanics-induced self-organization based on the concept of hyper-restoration (Beloussov, 2012; Igamberdiev, 2012). Other authors have devised parsimonious theories of embryogenesis whereby mechanical factors play a central role -if not the main role- in cell fate and thus tissue segmentation. For instance, in their theory of differentiation waves (Gordon, 1999; Gordon, N.K., and Gordon R., 2016), the authors consider the tug of war played between microfilament rings and microtubules mat at the apical end of epithelial cells. The microfilament rings foster cell contraction while the microtubules promote cell expansion. The mechanical equilibrium state is a metastable one and small mechanical perturbations can lead to a contracted or an expanded apex leading to specific gene networks being turned on or off, and thus to distinct cell fates. The new cell phenotype can itself be a source of mechanical perturbation and the process can re-iterate itself leading to a propagating differentiation wave. From the biomechanical perspective, the top-down causative role of mechanical stress can be assessed by the fact that membrane deformations due to external loads can trigger a cascade of cell processes that include mecanotransduction, gene transcription and translation (Gilmour et al., 2017). These mecano-chemical processes play a role in the control of differentiation, proliferation and other cell development stages and as well as in pathogenesis (Adjei and Blanka, 2015). The mechanical properties of living tissues combine ECM and cells' mechanical attributes that in turn depend on their molecular constituents. Collagen is the main structural macromolecule of the ECM and correlates with tissue strength. Elastin provides the elastic properties of connective tissues, and cadherins are transmembrane proteins that play an important role in adherens junctions that bind cells together. The combination of these molecular species (and others) gives the viscoelastic quality of living tissues. Cells in themselves can be considered as quasi-fluids that collectively will convey different properties if they form adherens junctions via cadherins or if they are mechanically independent from one another. During morphogenesis, both the ECM, cell lineages, and their collective organization change over time (e.g. the doing and undoing of adherens junctions), hence intrinsic mechanical properties also change over time and detailed multi-scale models of tissue biomechanics seems out of reach for now. The most widespread method used for studying deformable objects is the Finite Element Method (FEM) that is based on a Lagrangian description of continuum mechanics equations (Zienkiewicz, 2005). One key problem of continuum mechanics is to compute the elastic stresses inside a deformed volumetric object. A deformation field $\mathbf{u} = (u(\mathbf{r}), v(\mathbf{r}), w(\mathbf{r}))^{\mathrm{T}}$ defines a map between any material point located at $\mathbf{r} = (x, y, z)^T$ in a reference model (usually the undeformed object) and its new position $\mathbf{r}+\mathbf{u}$ in the deformed object. The Jacobian of the mapping between $\mathbf{r}$ and $\mathbf{r}+\mathbf{u}$ is given by $\mathbf{J} = \mathbf{I} + \nabla \mathbf{u}^T$. Using the Jacobian, the strain tensor $\boldsymbol{\varepsilon}$, can be computed either by using the non-linear Green-Saint-Venant formulation $\boldsymbol{\varepsilon} = \mathbf{J}^T\mathbf{J} - \mathbf{I}$, or the linear Cauchy Green formulation $\boldsymbol{\varepsilon} = \mathbf{J}^T\mathbf{J} - \mathbf{I}$ (Becker et al., 2009).

For linear and isotropic elastic material, the strain $\boldsymbol{\varepsilon}$ is related to the stress $\boldsymbol{\sigma}$ by Hooke's law:

$$\boldsymbol{\sigma} = \mathbf{C}\boldsymbol{\varepsilon} \tag{14}$$

where $\mathbf{C}$ is a rank four tensor, and both $\boldsymbol{\sigma}$ and $\boldsymbol{\varepsilon}$ are symmetric 3 × 3 (rank two) tensors. The diagonal element σ_{ii} of the stress tensor $\boldsymbol{\sigma}$, is the normal stress in the i^{th} direction while the non-diagonal elements σ_{ij} is the shear stress applied to a surface element i in the j^{th} direction. $\mathbf{C}$ characterizes the material "stiffness" and for an isotropic material depends on two coefficients: Young's Modulus E and Poisson's Ratio ν. The elastic force per unit volume at point **r** is computed in terms of the negative directional derivative along **u** of the strain energy density $U = (1/2)(\boldsymbol{\sigma}.\boldsymbol{\varepsilon})$:

$$\mathbf{f}(\mathbf{r}) = -\frac{1}{2}\nabla_{\mathbf{u}} U = -\boldsymbol{\sigma}\nabla_{\mathbf{u}}\boldsymbol{\varepsilon} \tag{15}$$

The stress tensor is real symmetric therefore there exists a rotation matrix $\mathbf{R}$ such that

$$\boldsymbol{\sigma}' = \mathbf{R}\boldsymbol{\sigma}\mathbf{R}^{T} = \begin{pmatrix} \sigma_1 & 0 & 0 \\ 0 & \sigma_2 & 0 \\ 0 & 0 & \sigma_3 \end{pmatrix} \tag{16}$$

where σ_i are the eigenvalues of the stress tensor and the corresponding eigenvectors denote the principal stress directions. $\boldsymbol{\sigma}$ and $\boldsymbol{\sigma}'$ denote the same physical reality represented in two coordinate systems that are rotated with respect to one another. Recent studies have shown that during collective cell migration, the cells' tend to coordinate their motions in order to transmit normal stress across cell-cell junctions while minimizing shear stress (Trepat and Fredberg, 2011). That is, cells migrate parallel to their respective first principal stress that is associated to the eigenvalue σ_1. The authors named this emergent collective behavior "plithotaxis" (from the Greek word "crowd"), that is distinct from chemotaxis or haptotaxis (Trepat and Fredberg, 2011).

Grid-based FEM are very popular among material and mechanical engineers (Zienkiewicz, 2005) yet they may not be the best suited for modeling large deformations of structures with highly complex and intertwined geometries with multi-phase interfaces; i.e. living tissues. In CM there is the additional complexity that all the structures of interest are evolving geometrically, topologically, and functionally over time. The smoothed Particle Hydrodynamic (SPH) and more generally particle based systems can provide some answers to these limitations. SPH is a Lagrangian meshless method that was initially designed to solve astrophysical problems (Gingold and Monaghan, 1977; Monaghan, 2005) and is gaining popularity in many areas of computational sciences, including Computational Fluid Dynamics (CFD) (Dalrymple and Rogers, 2006), magneto-hydrodynamics (Cerqueira and De Gouveia Dal Pino, 2001), solid mechanics (Bonet and Kulasegaram, 2000), and computer graphics (Desbrun and Gascuel, 1996; Müller et al., 2003; Becker et al., 2009). SPH is based on interpolation theory that approximates continuous field quantities by a disordered set of interpolation "particles". An SPH "particle" does not necessarily designates discrete entities but rather regional field quantities. In CM, quantities of interest include molecular concentrations, pressure, cell mass densities, ECM mass densities and mechanical stresses. The method allows any function to be expressed in terms of its values at a set of points representing particle positions using

a symmetrical smoothing kernel function (Gingold and Monaghan, 1977; Monaghan, 2005). The integral interpolant of any function $A(\mathbf{r})$ is defined by

$$A(\mathbf{r}) = \int A(\mathbf{r}')W(\mathbf{r} - \mathbf{r}', h)\, d\mathbf{r}' \tag{17}$$

where W is a radial symmetrical smoothing kernel and the smoothing length h represents the compact support of the kernel that ensures zero interactions outside their computational range. That is, each particle *i* only interacts with the set N_i of neighboring particles that are within the radius h of *i* which reduces the computational load. The numerical approximation of the integral interpolant is given by

$$A_s(\mathbf{r}) = \sum_{j \in N_i} A_j W(\mathbf{r}_i - \mathbf{r}_j, h) V_j \tag{18}$$

where V_j is the volume attributed to particle j. In the case of real material such as fluids and viscoelastic material such as cells, a particle *j* has a mass m_j and a mass density ρ, and (eq. 18) becomes

$$A_s(\mathbf{r}) = \sum_{j \in N_i} A_j \frac{m_j}{\rho_j} W(\mathbf{r}_i - \mathbf{r}_j, h) \tag{19}$$

Using SPH, derivatives in constitutive laws are computed by shifting the differential operator to the kernel function. The gradient and Laplacian of $\boldsymbol{A}$ can be derived straightforwardly from (eq. 19)

$$\nabla A_s(\mathbf{r}) = \sum_j A_j \frac{m_j}{\rho_j} \nabla W(\mathbf{r}_i - \mathbf{r}_j, h) \tag{20}$$

$$\nabla^2 A_s(\mathbf{r}) = \sum_j A_j \frac{m_j}{\rho_j} \nabla^2 W(\mathbf{r}_i - \mathbf{r}_j, h) \tag{21}$$

Isothermal mass densities can be obtained from (eq. 19)

$$\rho(\mathbf{r}_i) = \sum_{j \in N_i} m_j W(\mathbf{r}_i - \mathbf{r}_j, h) \tag{22}$$

The starting point of an SPH-based study of viscoelastic material is the Navier-Stokes eq.(4) that combines a pressure-gradient force, a viscous force and an external force.

The pressure that results in purely repulsive forces can be derived from the ideal gas equation (Müller et al., 2003)

$$p\left(\mathbf{r}_i\right) = k\rho\left(\mathbf{r}_i\right) \tag{23}$$

A modified version accounts for particle cohesion by introducing a rest density (Desbrun and Gascuel, 1996):

$$p\left(\mathbf{r}_i\right) = k\left(\rho\left(\mathbf{r}_i\right) - \rho_0\right) \tag{24}$$

This relation can be applied for tissues made of cells that have formed adherens junctions for instance. A negative pressure will correspond to a stretched material (tensile stress) while a positive value to a compressed one (compressive stress). The coefficient k can be viewed as a "stiffness" factor and adjacent tissue regions with distinct stiffnesses will be assigned different k values.

An asymmetric pressure-gradient force can be obtained by combining the pressure term of Navier-Stokes (eq. 4) with (eq. 20):

$$\mathbf{f}_{press}\left(\mathbf{r}_i\right) = -\nabla p\left(\mathbf{r}_i\right) = -\sum_{j\in N_i} p_j \frac{m_j}{\rho_j} \nabla W\left(\mathbf{r}_i - \mathbf{r}_j, h\right) \tag{25}$$

and be symmetrized (Müller et al., 2003):

$$\mathbf{f}_{press}\left(\mathbf{r}_i\right) = -\nabla p\left(\mathbf{r}_i\right) = -\sum_{j\in N_i} m_j \frac{p_i + p_j}{\rho_j} \nabla W\left(\mathbf{r}_i - \mathbf{r}_j, h\right) \tag{26}$$

Likewise, an asymmetric viscous force can be obtained by combining the viscous term of the Navier-Stokes (eq. 4) with (eq. 21):

$$\mathbf{f}_{visc}\left(\mathbf{r}_i\right) = \upsilon\nabla^2\mathbf{v}\left(\mathbf{r}_i\right) = \upsilon\sum_{j\in N_i} \mathbf{v}_j \frac{m_j}{\rho_j} \nabla^2 W\left(\mathbf{r}_i - \mathbf{r}_j, h\right) \tag{27}$$

and be symmetrized (Müller et al., 2003):

$$\mathbf{f}_{visc}\left(\mathbf{r}_i\right) = \upsilon\nabla^2\mathbf{v}\left(\mathbf{r}_i\right) = \upsilon\sum_{j\in N_i} m_j \frac{\mathbf{v}_j - \mathbf{v}_i}{\rho_j} \nabla^2 W\left(\mathbf{r}_i - \mathbf{r}_j, h\right) \tag{28}$$

The external force $\mathbf{f}_{ext}$ of (eq. 4) typically incorporates gravity. When we model cells or a part thereof as particles we combine features of the Discrete Elements Method (166) with the "soft" SPH interactions. Cell-cell adhesion between cells forming adherens junctions is modeled by adding springs between the neighboring particles. Elastic forces between particles *i* and *j* is the spring equivalent of Hookean continuous material (eqs. 14 &15).

$$\mathbf{f}_{elast}\left(\mathbf{r}_i,\mathbf{r}_j\right)=C_{adh}\left(\left(\mathbf{u}^T\mathbf{u}\right)^{\frac{1}{2}}-d_{rest}\right)\frac{\mathbf{u}}{\|\mathbf{u}\|} \qquad (29)$$

were $\mathbf{u}=\mathbf{r}_i-\mathbf{r}_j$, and d_{rest} is the cell's resting diameter and C_{adh} the cell-cell spring stiffness. This is a rather simple method for approximating the cellular contribution to tissue elasticity and more elaborate (but more time-consuming) methods based on deformation fields, stress and strain tensors (eqs 14 & 15) can be easily be implemented, e.g. (Becker et al., 2009).

Cell-ECM adhesion for kinematically quiescent cells is modeled by adding a spring that link the cell to the ECM. The elastic force between a particle *i* and the ECM is given by the following rule:

$$\mathbf{f}_{ecm}\left(\mathbf{r}_i,\mathbf{r}_{rest}\right)=C'\left(\mathbf{u}^T\mathbf{u}\right)^{\frac{1}{2}}\frac{\mathbf{u}}{\|\mathbf{u}\|} \quad \text{if} \quad \|\mathbf{f}_{ecm}\|\le\lambda_{adh}^{ecm} \qquad (30)$$

o otherwise

where $\mathbf{u}=\mathbf{r}_i-\mathbf{r}_{rest}$, and $\mathbf{r}_{rest}$ is the resting position, λ_{adh}^{ecm} is the threshold force beyond which the cell loses "grip" of the matrix, and C' is the cell-ECM spring stiffness.

4.5. Combining chemical, mechanical and electric fields

The formation of lumen space (sect.2.7) can be simulated at the microscopic scale where, in our case, a cell is represented by a single SPH particle. Epithelial cell condensation due to chemical morphogens, planar cell polarity and epithelial adherens junctions are the preliminary events that must be simulated first. This results in vesicle or chord-like condensates of polarized cells forming a proto-lumen. In the GMSP, lumen formation can be modeled as a cavitation process as as well as by epithelial cell separation. In epithelial cell separation, lumen space is created by ATP-dependent Na^+ influx that results in an increased lumen Na^+ concentration. The difference in sodium concentration between the nascent lumen and mesenchyme compartments results in osmotic forces that drive water molecules to move from the mesenchyme into the lumen until the sodium concentrations equilibrate. The osmotic pressure is mathematically expressed by van't Hoff's equation: $\Pi = C_{Na}RT = \alpha C_{Na}$, where C_{Na} is the sodium molar concentration. Molar concentrations can be reformulated in terms of mass densities using Avogadro's number and the atomic mass. The increase

in lumen water density due to the increase of lumen sodium density can then be deduced by the equating Na^+/H_20 equilibrium ratios before and after osmosis leading to the following expression:

$$\rho_w = \rho_w^0 \left(1 + \frac{\Delta \rho_{Na}}{\rho_{Na}^0} \right) \tag{31}$$

where ρ_{Na}^0 and ρ_w^0 are the reference interstitial sodium and water densities. In SPH context, osmosis can be modeled by creating a water source at the proto-lumen center that increases the lumen water mass density (eq. 21) resulting in a positive lumen hydrostatic pressure (eq. 23) and a lumen-to-mesenchyme net pressure-gradient force $\mathbf{f}_{\text{osm}}$ (eq. 25) "perceived" by the epithelial cells. In addition, if negatively charged proteoglycans at the cells' apical domains are to be accounted for (sect. 2.8), then electrostatic forces must also be factored in. Assuming that the net apical charge for a given cell at position $\mathbf{r}_i$ is $-q$, then the electrostatic force at the charge position due to the surrounding electric field is given by $\mathbf{f}_E(\mathbf{r}_i) = -q\mathbf{E}(\mathbf{r}_i)$. The electric field at the charge position results from the combined contributions of epithelial membrane potentials (eq. 13) and the field produced by the negative apical charges of the other particles positioned at $\mathbf{r}_j \neq \mathbf{r}_i$. When cells migrate during cell sorting and cell condensation (sect.2.3), or during duct elongation and cell intercalation (sect. 2.5) cell-matrix adhesion and cyclic cell protrusions and contractions produces a force exerted by the cell on the matrix that results in an equal and opposite traction force applied by the ECM on cell (Newton's 3rd law). Our cell migration model, which covers chemotaxis and haptotaxis is reduced to a simple form since the complex cell-ECM interactions resulting from cyclic adhesion, protrusions, and contraction phases are summed-up in a single traction force that is proportional to a chemical and/or electric field gradient: $\mathbf{f}_{migr}(u, \mathbf{r}_i) = \beta \nabla u$.

4.6. Equations of motion

The net force perceived by a cell that cause its repositioning follows the equation of motion.

$$\mathbf{f}_{total}(\mathbf{r}_i) = \mathbf{f}_{press}(\mathbf{r}_i) + \mathbf{f}_{visc}(\mathbf{r}_i) + \mathbf{f}_{elast}(\mathbf{r}_i) + \mathbf{f}_{osm}(\mathbf{r}_i) + \mathbf{f}_{ecm}(\mathbf{r}_i) + \mathbf{f}_E(\mathbf{r}_i) + \mathbf{f}_{migr}(u, \mathbf{r}_i) \tag{32}$$

$$\mathbf{v}_i(t + \Delta t) = \frac{\mathbf{f}_{total}}{\mathrm{m}_i} \Delta \mathrm{t} \tag{33}$$

$$\mathbf{r}_i(t + \Delta t) = \mathbf{r}_i(t) + \mathbf{v}_i(t + \Delta t)\Delta t \tag{34}$$

When mechanical equilibrium is reached then the actual cell shapes can be approximated by a Voronoi tesselation.

5. Discussion and conclusion

Morphogenesis vividly illustrates the profound link between form and function in biology. It arises from the integration of coupled chemical, electrical and mechanical processes that operate across multiple spatial and temporal scales. These processes can be represented by a small number of constitutive equations that can be derived from even fewer first principles like the conservation of momentum. The scope of constitutive equations is very broad since they can model molecular as well as galactic-scale phenomena and their generality is a witness of the deep unity that prevails in the universe as well as the universality of the mathematical language. Since constitutive equations cover abiotic as well as biological phenomena, some pending questions remain: what factors distinguishes the two and how can they be incorporated within a single computational framework? The most obvious differentiating factor is the living cell and its constant adaptation to external cues (see Part II of this special issue). Intra and intercellular communication fields permeate biological tissues, but their spatiotemporal patterns are constantly changing in shape, modality and intensity due to the cells' activities that are governed by the expression of their genes. It is the simultaneous top-down (environment to genes) and bottom-up (gene-to-environment) cross-talks that determines the development, growth and livelihood of organisms. Figures 1-4 and figs. 6-7 summarize some of the results obtained when cells coordinate their actions via multimodal interactions that can be modeled by constitutive equations. However, such equations are ill-suited to capture the reactivity and goal-driven behavior of living cells and organisms in general, and this topic will be described in Part II. The results that we have obtained thus far have been satisfactory in a *qualitative sense only* and insofar as the generated models share common structural and functional features with the target objects to be modeled. We have not yet matched the models with detailed data and these preliminary results have only concluded a feasibility study with an early-stage prototype. Substantial and long-term additional work is needed to improve all phases of the modeling task. For instance a pending question that needs to be addressed is the following: since all constitutive laws are computed by shifting the differential operators to the kernel function, chemical advection and diffusion, as well as electric, magnetic and electromagnetic potentials and fields can, at least in theory, be computed by the SPH approach. There are good reasons to explore the benefits that could be drawn from having a unique formalism for all the modalities. Other directions of research areas include developing a more rigorous approach to biomechanics with the explicit inclusion of the ECM, implementing a full integration of the bidomain theory to biolelectric extra-cellular fields (currently monodomain approximation), integrating and carrying-out benchmarking studies between multimodal all mesh-free (Lagrangian) particle-based modeling, all grid-based (Eulerian) modeling, and mixed approaches (as we have now). Last but not least, a CM platform can be operational only if it is implemented on high-performance computing infrastructures, which means adapting the code to these types of infrastructures.

6. References

Adams, D.S., Levin, M., 2013. Endogenous voltage gradients as mediators of cell-cell communication: strategies for investigating bioelectrical signals during pattern formation. Cell Tissue Res. 352, 95-122.

Adams, D. S., Robinson, K. R., Fukumoto, T., Yuan, S., Albertson, R.C., Yelick, P., Kuo, L., McSweeney, M., Levin, M., 2006. Early, H+-V-ATPase-dependent proton flux is necessary for consistent left-right patterning of non-mammalian vertebrates. Development 133(9), 1657-1671. https://doi:10.1242/dev.02341.

Adjei, I.M., Blanka, S., 2015. Modulation of the Tumor Microenvironment for Cancer Treatment: A Biomaterials Approach. J. Funct. Biomater. 6(1), 81-103.

Anderson, A.R.A, Weaver, A.M., Cummings, P.T., Quaranta, V., 2006. Tumor Morphology and Phenotypic Evolution Driven by Selective Pressure from the Microenvironment. Cell 127, 905-915.

Arcangeli, A., Crociani, O., Lastraioli, E., Masi, A., Pillozzi, S., Becchetti, A., 2009. Targeting ion channels in cancer: a novel frontier in antineoplastic therapy. Curr. Med. Chem. 16, 66-93. https://doi:10.2174/09298670978700.

Axelrod, J.D., Bergmann, D.C., 2014. Coordinating cell polarity: heading in the right direction? Development 141, 3298-3302.

Bandini, S., Mauri, G., 1999. Multilayered cellular automata. Theor. Comput. Sci. 217(1), 99-113.

Bard, J., Ross, A., 1982. The morphogenesis of the ciliary body of the avian eye: II. Differential enlargement causes an epithelium to form radial folds. Dev. Bio. 92 (1), 87-96.

Bauer, B., Siebert, R., Traulsen, A., 2015. Cancer initiation with epistatic interactions between driver and passenger mutations. J. Theor. Biol. 358, 52–60.

Beane, W.S., Morokuma, J., Lemire, J.M., Levin, M., 2013. Bioelectric signaling regulates head and organ size during planarian regeneration. Development, 140, 313–322. https://doi:10.1242/dev.086900.

Becker, M., Ihmsen, M., Teschner, M., 2009. Corotated SPH for Deformable Solids. In: Proc. 5th Eurographics Workshop on Natural Phenomena. The Eurographics Association. E. Galin and J. Schneider (Editors), pp 27-34. https://doi:10.2312/EG/DL/conf/EG2009/nph/027-034.

Beloussov, L.V., 2012. Morphogenesis as a macroscopic self-organizing process. Biosystems, 109(3), 262–279.

Bergstralh, D.T., Haack, T., St Johnston, D., 2013. Epithelial polarity and spindle orientation: intersecting pathways. Philos. Trans. R. Soc. Lond. B Biol. Sci. 368(1629), 20130291. https://doi:10.1098/rstb.2013.0291.

Bonet, J., Kulasegaram, S., 2000. Corrections and stabilization of Smooth Particle Hydrodynamics methods with applications in metal forming simulations. Int. J. Numer. Methods. Eng. 47(6), 1189–1214.

Catterall, W.A., Raman, I.M., Robinson, H.P.C., Terrence, J., Sejnowski, T.J., Paulsen, O., 2012. The Hodgkin-Huxley Heritage: From Channels to Circuits. J. Neurosci. 32(41), 14064-14073. https://doi:10.1523/JNEUROSCI.3403-12.2012.

Cerqueira, A.H., De Gouveia Dal Pino, E., 2001. Three-dimensional magnetohydrodynamic simulations of radiatively cooling pulsed jets. Astrophys. J. 560, 779-791. https://doi.org/10.1086/322245.

Chaouiya, C., 2007. Petri net modelling of biological networks. Brief. Bioinform. 8(4), 210–219.

Chen, D., Jiao Y., Torquato S., 2014. A Cellular Automaton Model for Tumor Dormancy: Emergence of a Proliferative Switch. PLoS ONE 9(10), e109934. https://doi:10.1371/journal.pone.0109934.

Chernet, B., Levin, M., 2013. Endogenous Voltage Potentials and the Microenvironment: Bioelectric Signals that Reveal, Induce and Normalize Cancer. J. Clin. Exp. Oncol. Suppl 1, S1-002.

Chmielecki, J., Foo, J., Oxnard, G.R., Hutchinson, K., et al. 2011. Optimization of dosing for EGFR mutant non-small cell lung cancer with evolutionary cancer modeling. Sci. Transl. Med. 3(90):90ra59. https://doi:10.1126/scitranslmed.3002356.

Costantini, F., Kopan, R., 2010. Patterning a Complex Organ: Branching Morphogenesis and Nephron Segmentation in Kidney Development. Dev. Cell. 18(5), 698-712. https://doi:10.1016/j.devcel.2010.04.008.

Cristini, V., Li, X., Lowengrub, J.S., Wise S.M., 2009. Nonlinear simulations of solid tumor growth using a mixture model: invasion and branching. J. Math. Biol. 58, 723–63.

Dalrymple, R. A., Rogers, B., 2006. Numerical modeling of water waves with the SPH method. Coastal Engineering 53, 141–147.

Dascalu, M., Stefan, G., Zafiu, A., Plavitu, A., 2011. Applications of multilevel cellular automata in epidemiology. In: Proceedings of the 13th WSEAS international conference on Automatic control, modelling & simulation. Ed., World Scientific and Engineering Academy and Society (WSEAS): 439-444.

Debnath, J., Mills, K.R., Collins, N.L., Reginato, M.J., Muthuswamy, S.K., Brugge, J.S., 2002. The Role of Apoptosis in Creating and Maintaining Luminal Space within Normal and Oncogene-Expressing Mammary Acini. Cell 111, 29–40.

Delile, J., Herrmann, M., Peyrieras, N., Doursat, R., 2017. A cell-based computational model of early embryogenesis coupling mechanical behavior and gene regulation. Nat. Commun. 8:13929. https://doi:10.1038ncomms13929.

De Pillis, L. G., Radunskaya, A., 2001. A mathematical tumor model with immune resistance and drug therapy: an optimal control approach. J. Theor. Med. 3(2), 79–100. http://dx.doi.org/10.1080/10273660108833067

Desbrun, M., Gascuel, M.P., 1996. Smoothed Particles: A new paradigm for animating highly deformable bodies. In: Boulic R., Hégron G. (eds) Comput. Anim. and Sim. '96, Eurographics. Springer, Vienna, pp 61–76. https://doi.org/10.1007/978-3-7091-7486-9_5.

Dewey, E.B., Taylor, D.T., Johnston, C.A., 2015. Cell Fate Decision Making through Oriented Cell Division. J. Dev. Biol. 3, 129-157.

DiFrancesco, D., Noble, D., 1985. A model of cardiac electrical activity incorporating ionic pumps and concentration changes. Philos. Trans. R. Soc. Lond. B Biol. Sci. 307(1133), 353-398.

Dillon, R.H., Hans, G., 1999. A mathematical model for outgrowth and spatial patterning of the vertebrate limb bud. J. Theor. Biol. 197, 295–330.

Duboc, V., Logan, M.P.O., 2009. Building limb morphology through integration of signaling modules. Curr. Opin. Genet. Dev. 19(5), 497–503. https://doi.org/10.1016/j.gde.2009.07.002.

Durant, F., Lobo, D., Hammelman, J., Levin, M., 2016. Physiological controls of large-scale patterning in planarian regeneration: a molecular and computational perspective on growth and form. Regeneration (Oxf) 3(2), 78-102. https://doi:10.1002/reg2.54.

Eisenhammer, T., Hubler, A., Packard, N., Kelso, J.A.S., 1991. Modeling experimental time series with ordinary differential equations. Biol. Cybern. 65(2), 107–112.

Ewald, A.J., Brenot, A., Duong, M., Chan, B.S., Werb, Z., 2008. Collective Epithelial Migration and Cell Rearrangements Drive Mammary Branching Morphogenesis. Dev. Cell. 14, 570–581.

Eyckmans, J., Chen, C.S., 2017. 3D culture models of tissues under tension. J. Cell Sci. 130, 63-70.

Fernandez, J., Zhang, J., Heidlauf, T., Sartori, M., Besier, T., Röhrle, O., Lloyd, D., 2016. Multiscale musculoskeletal modelling, data–model fusion and electromyography-informed modelling. Interface Focus 6:20150084. https://doi:10.1098/rsfs.2015.0084.

Fletcher, A.G., Osterfield, M., Baker, R.E., Shvartsman, S.Y., 2014. Vertex models of epithelial morphogenesis. Biophys. J., 106, 2291–2304.

Formosa-Jordan, P., Ibanes, M., Ares, S., Frade, J.M., 2013. Lateral inhibition and neurogenesis: novel aspects in motion. Int. J. Dev. Biol. 57, 341-350.

Fraser, S.P., Ozerlat-Gunduz, I., Brackenbury, W.J., Fitzgerald, E.M., Campbell, T.M., Coombes, R.C., Djamgoz, M.B.A., 2014. Regulation of voltage-gated sodium channel expression in cancer: hormones, growth factors and auto-regulation. Philos. Trans. R. Soc. Lond. B Biol. Sci. 369, 20130105.

Frenz, D.A., Jaikaria, N.S., Newman, S.A., 1989. The mechanism of precartilage mesenchymal condensation: a major role for interaction of the cell surface with the amino-terminal heparin-binding domain of fibronectin. Dev. Biol. 136, 97–103.

Funk, R.H.W., 2015. Endogenous electric fields as guiding cue for cell migration. Front. Physiol. 6, 143. https://doi: 10.3389/fphys.2015.00143.

Gao, R. C., Zhang, X. D., Sun, Y. H., Kamimura, Y., Mogilner, A., Devreotes, P. N., Zhao, M., 2011. Different roles of Membrane potentials in electrotaxis and chemotaxis of Dictyostelium Cells. Eukaryot. Cell 10, 1251–1256.

Gevertz, J.L., Torquato, S., 2006. Modeling the effects of vasculature evolution on early brain tumor growth. J. Theor. Biol. 243, 517–531.

Gierer, A., 1981. Generation of biological patterns and form: some physical, mathematical, and logical aspects. Prog. Biophys. molec. Biol. 37, 1-47.

Gierer, A., Meinhardt, H., 1972. A theory of biological pattern formation. Kybernetik 12, 30-39.

Gilmour, D., Rembold, M., Leptin, M., 2017. From morphogen to morphogenesis and back. Nature 541, 311–320.

Gingold, R.A., Monaghan, J.J., 1977. Smoothed particle hydrodynamics theory and application to non-spherical stars. Mon. Not. R. Astron. Soc. 181, 375–389.

Glazier, J.A., Graner, F., 1993. Simulation of the differential adhesion driven rearrangement of biological cells. Phys. Rev. E, 47, 2128–2154. https://doi.org/10.1103/PhysRevE.47.2128.

Gordon, R., 1999. The Hierarchical Genome and Differentiation Waves: Novel Unification of Development, Genetics and Evolution. Singapore & London, World Scientific & Imperial College Press.

Gordon, N.K., Gordon R., 2016. The organelle of differentiation in embryos: the cell state splitter [invited review]. *Theoretical Biology and Medical Modelling* **13**(Special issue: Biophysical Models of Cell Behavior, Guest Editor: Jack A. Tuszynski), #11.

Graner, F., Glazier, J.A., 1992. Simulation of biological cell sorting using a two-dimensional extended Potts model. Phys. Rev. Lett. 69, 2013–2016.

Gunji, Y.P., Ono, R., 2012. Sociality of an agent during morphogenetic canalization: Asynchronous updating with potential resonance. Biosystems 109, 420–429.

Gupta, P.B., Fillmore, C.M., Jiang, G., Shapira, S.D., Tao, K., Kuperwasser, C., Lander, E.S., 2009. Stochastic State Transitions Give Rise to Phenotypic Equilibrium in Populations of Cancer Cells. Cell 146, 633–644.

Hall, B.K., Miyake, T., 2000. All for one and one for all: condensations and the initiation of skeletal development. Bioessays 22, 138–147.

Hebner, C., Weaver, V.M., Debnath, J., 2008. Modeling Morphogenesis and Oncogenesis in Three-Dimensional Breast Epithelial Culture. Annu. Rev. Pathol. Mech. Dis. 3, 313–39.

Henriquez, C.S., 1993. Simulating the electrical behavior of cardiac tissue using the bidomain model. Crit. Rev. Biomed. Eng., 21(1), 1-77.

Hiscock, T.W., Megason, S.G., 2015. Orientation of Turing-like Patterns by Morphogen Gradients and Tissue Anisotropies. Cell Systems 1, 408–416.

Höckel, M., 2015. Morphogenetic fields of embryonic development in locoregional cancer spread. Lancet Oncol. 16, e148–e151.

Hodgkin, A.L., Huxley, A.F., 1952. A quantitative description of membrane current and its application to conduction and excitation in nerve. J. Physiol. 117(4), 500-544.

Honda, H., Tanemura, M., Yoshida, A., 2000. Differentiation of wing epidermal scale cells in a butterfly under the lateral inhibition model—Appearance of large cells in a polygonal pattern. Acta Biotheor. 48, 121-136.

Howard, B.A, Gusterson, B.A., 2000. Human Breast Development. J. Mammary Gland Biol. Neoplasia 5, 119-137.

Iber, D., Tanaka, S., Fried, P., Germann, P., Menshykau, D., 2015. Simulating tissue morphogenesis and signaling. Methods Mol. Biol. 1189, 323–338.

Igamberdiev, A.U., 2012. Biomechanical and coherent phenomena in morphogenetic relaxation processes. Biosystems 109, 336–345.

Jacobson, A.G., Gordon R., 1976. Changes in the shape of the developing vertebrae nervous system analyzed experimentally, mathematically and by computer simulation, J. Exp. Zool. 197(2), 191-246.

Karner, C.M., Chirumamilla, R., Aoki, S., Igarashi, P., Wallingford, J.B., Carroll, T.J., 2009. Wnt9b signaling regulates planar cell polarity and kidney tubule morphogenesis. Nat. Genet. 41(7), 793–799.

Kim, Y., Othmer, H.G., 2013. A hybrid model of tumor-stromal interactions in breast cancer. Bull. Math. Boil. 75, 1304–1350.

Kondo, S., Miura, T., 2010. Reaction-diffusion model as a framework for understanding biological pattern formation. Science 329, 1616-1620.

Krause, M., Rak-Raszewska, A., Pietilä, I., Quaggin, S.E., Vainio S., 2015. Signaling during Kidney Development. Cells 4, 112-132.

Lang, F., Foller, M., Lang, K.S., Lang, P.A., Ritter, M., Gulbins, E., Vereninov, A., Huber, S.M., 2005. Ion channels in cell proliferation and apoptotic cell death. J. Membr. Biol. 205, 147–157.

Law, R., Levin M., 2015. Bioelectric memory: modeling resting potential bistability in amphibian embryos and mammalian cells. Theor. Biol. Med. Model. 12:22. https://doi:10.1186/s12976-015-0019-9.

Levin, M., 2012. Morphogenetic fields in embryogenesis, regeneration, and cancer: non-local control of complex patterning. Biosystems 109(3), 243-61. https://doi: 10.1016/j.biosystems.2012.04.005.

Levin, M., 2014. Molecular bioelectricity: how endogenous voltage potentials control cell behavior and instruct pattern regulation in vivo. Mol. Biol. Cell. 25(24), 3835-5380.

Li, J.F., Lowengrub, J., 2014. The effects of cell compressibility, motility and contact inhibition on the growth of tumor cell clusters using the Cellular Potts Model. J. Theor. Biol. 343, 79–91.

Lienkamp, S., Liu, K., Karner, C.M., Carroll, T.J., Ronneberger, O., Wallingford, J.B., Walz G., 2012. Vertebrate kidney tubules elongate using a planar cell polarity dependent, rosette-based mechanism of convergent extension. Nat. Genet. 44(12), 1382–1387. https://doi:10.1038/ng.2452.

Lopez Rincon, A., Shimoda, S., 2016. The inverse problem in electroencephalography using the bidomain model of electrical activity. J. Neurosci. Methods 274, 94-105. https://doi.org/10.1016/j.jneumeth.2016.09.011.

Lowengrub, J.S., Frieboes, H.B., Jin, F., Chuang, Y.L., Li, X., Macklin, P., Wise, S.M., Cristini V., 2010. Nonlinear modeling of cancer: Bridging the gap between cells and tumors. Nonlinearity 23(1), R1–R9.

Macara, I.G., McCaffrey, L., 2013. Cell polarity in morphogenesis and metastasis. Philos. Trans. R. Soc. Lond. B Biol. Sci. 368, 2013001.

Macias, H., Hinck, L., 2012. Mammary gland development. Wiley Interdiscip. Rev. Dev. Biol. 1(4), 533-557. https://doi: 10.1002/wdev.35.

Macklin, P., Lowengrub, J.S., 2008. A new ghost cell/level set method for moving boundary problems: application to tumor growth. J. Sci. Comput. 35 (2-3), 266–299. https://doi:10.1007/s10915-008-9190-z.

Mammoto, T., Mammoto, A., Torisawa, Y.S., Tat ,T., Gibbs, A., Derda, R., Mannix, R., de Bruijn, M., Yung, C.W., Huh, D., Ingber, D.E., 2011. Mechanochemical control of mesenchymal condensation and embryonic tooth organ formation. Dev. Cell. 21(4), 758–769.

Martín-Belmonte, F., Yu, W., Rodríguez-Fraticelli, A.E., Ewald, A., Werb, Z., Alonso, M.A., Mostov, K. 2008. Cell-Polarity Dynamics Controls the Mechanism of Lumen Formation in Epithelial Morphogenesis. Curr. Biol. 18, 507–513.

Maung, S.M.T.W., Jenny, A., 2011. Planar cell polarity in Drosophila. Organogenesis 7(3), 165-179.

McBeath, R., Pirone, D.M., Nelson, C.M., Bhadriraju, K., Chen, C.S., 2004. Cell shape, cytoskeletal tension, and RhoA regulate stem cell lineage commitment. Dev. Cell. 6, 483–495.

Meineke, F.A., Potten, C.S., Loeffler, M., 2001. Cell migration and organization in the intestinal crypt using a lattice-free model. Cell Prolif. 34, 253–266.

Meinhardt, H., 2008. Models of biological pattern formation: from elementary steps to the organization of embryonic axes. Curr. Top. Dev. Biol. 81, 1-63.

Menshykau, D., Erkan Ünal, P.B., Sapin, V., Iber, D., 2014. An interplay of geometry and signaling enables robust lung branching morphogenesis. Development, 141, 4526-4536.

Meyers, L.A., Pourbohloul, B., Newman, M.E, Skowronski, D.M., Brunham, R.C., 2005. Network theory and SARS: predicting outbreak diversity. J. Theor. Biol., 232, 71-81.

Monaghan, J.J., 2005. Smoothed Particle Hydrodynamics. Rep. Prog. Phys. 68(8), 1703-1759. https://doi.org/10.1088/0034-4885/68/8/R01.

Müller, M., Charypar, D., Gross, M., 2003. Particle based fluid simulation for interactive applications. In Proceedings of the 2003 ACM SIGGRAPH/Eurographics symposium on Computer animation, 154-159.

Munoz, J.J., Conte, V., Miodownik, M., 2010. Stress-dependent morphogenesis: Continuum mechanics and truss systems. Biomech. Model. Mechanobiol. 9, 451-467.

Navis, A., Nelson, C.M., 2016. Pulling together: Tissue-generated forces that drive lumen morphogenesis. Semin. Cell. Dev. Biol. 55, 139-147.

Nerurkar, N.L., Mahadevan, L., Tabin, C.J., 2016. BMP signaling controls buckling forces to modulate looping morphogenesis of the gut. Proc. Natl. Acad. Sci. U. S. A., 114, 2277-2282.

Nigam, S.K., Shah, M.M., 2009. How Does the Ureteric Bud Branch? J. Am. Soc. Nephrol. 20, 1465-1469.

Nishimura, T., Takeichi, M., 2008. Shroom3-mediated recruitment of Rho kinases to the apical cell junctions regulates epithelial and neuroepithelial planar remodeling. Development 135, 1493-1502. doi:10.1242/dev.019646.

Noble, D., 1962. A modification of the hodgkin-huxley equation applicable to Purkinje fibre action and pacemaker potentials. J. Physiol. 160, 317–352.

Noble, D., 2012. A theory of biological relativity: no privileged level of causation. Interface Focus 2, 55–64.

Oberlender, S.A., Tuan, R.S., 1994. Expression and functional involvement of N-cadherin in embryonic limb chondrogenesis. Development 120, 177–187.

Painter, K.J, 2009. Continuous Models for Cell Migration in Tissues and Applications to Cell Sorting via Differential Chemotaxis. Bull. Math. Biol. 71(5), 1117–1147. https://doi: 10.1007/s11538-009-9396-8.

Pan, F.C., Wright, C., 2011. Pancreas Organogenesis: From Bud to Plexus to Gland. Dev. Dyn. 240, 530-565.

Pearson, J.F., Hughes, S., Chambers, K., Lang, S.H., 2009. Polarized fluid movement, and not cell death creates luminal spaces in adult prostate epithelium. Cell Death Differ. 16(3), 475–482.

Peng, H., Zhao, W., Tanetal, H., 2016. Prediction of treatment efficacy for prostate cancer using a mathematical model. Scientific Reports 6, Article ID 21599. https://doi:10.1038/srep21599.

Pezzuto, S., Kal'avský, P., Potse, M., Prinzen, F.W., Auricchio, A., Krause, R., 2017. Evaluation of a Rapid Anisotropic Model for ECG Simulation. Front. Physiol. 8, 265. https://doi:10.3389/fphys.2017.00265

Piotrowska, M.J., Angus, S.D., 2009. A quantitative cellular automaton model of in vitro multicellular spheroid tumour growth. J. Theor. Biol. 258, 165–78.

Portegys, T., Pascualy, G., Gordon, R., McGrew, S.P., Alicea, B. , 2016. Morphozoic, Cellular Automata with Nested Neighborhoods as a Metamorphic Representation of Morphogenesis, [invited]. In:Multi-Agent Based Simulations Applied to Biological and Environmental Systems. D.F. Adamatti, (ed.) IGI Global: pp. 44-80.

Prigogine, I., Stengers, I., 1979. La Nouvelle Alliance, Gallimard, Paris.

Ragkousi, K., Gibson, M.C., 2014. Cell division and the maintenance of epithelial order. J. Cell Biol. 207(2), 181–188.

Rejniak, K.A., 2007. An immersed boundary framework for modelling the growth of individual cells: An application to the early tumor development. J. Theor. Biol. 247, 186–204.

Rejniak, K.A., Dillon, R.H., 2007. A single-cell-based model of the ductal tumour microarchitecture. Comput. Math. Methods Med. 8(1), 51-69.

Sachs, N., Tsukamoto, Y., Kujala, P., Peters, P.J., Clevers H., 2017. Intestinal epithelial organoids fuse to form self-organizing tubes in floating collagen gels. Development 144, 1107-1112.

Saez-Rodriguez, J., Alexopoulos, L.G., Epperlein, J., Alexopoulos, L.G., Epperlein, J., Samaga, R., Lauffenburger, D.A., Klamt, S., Sorger, P.K., 2009. Discrete logic modelling as a means to link protein signaling networks with functional analysis of mammalian signal transduction. Mol. Syst. Biol. 5, 331. https://doi:10.1038/msb.2009.87.

Savin, T., Kurpios, N.A., Shyer, A.E., Florescu, P., Liang, H., Mahadevan, L., Tabin, C. J., 2011. On the growth and form of the gut. Nature 476, 57–62.

Shi, Y., Yao, J., Xu, G., Taber, L.A., 2014. Bending of the looping heart: differential growth revisited. J. Biomech. Eng. 136, 1–15.

Shih, H.P., Panlasigui, D., Cirulli, V., Sander, M., 2016. ECM signaling regulates collective cellular dynamics to control pancreas branching morphogenesis. Cell Rep. 14(2), 169–179.

Shih, H.P., Wang, A., Sander, M., 2013. Pancreas Organogenesis: From lineage determination to morphogenesis. Annu. Rev. Cell Dev. Biol. 29, 81-105. https://doi:10.1146/annurev-cellbio-101512-122405.

Siregar, P., 1996a. Theoretical Cardiology: From Mathematical to Qualitative Models. J. Biol. Sys. 4, 131-150.

Siregar, P., 2000. Method for three-dimensional construction of a virtual organ representing a real organ. European patent WO 2000072272 A1.

Siregar, P., 2009. Simulation of complex Systems. European Patent n° 08290535.7.

Siregar, P., Chahine, M., Lemoulec, F., Le Beux, P., 1995. An Interactive Qualitative Model in Cardiology. Comput. Biomed. Res., 28, 443-478.

Siregar, P., Julen, N., Sinteff, J.P., 2003. Computational Integrative Physiology: At the Convergence of the Life, Physical and Computational Sciences. Meth. Inform. Med. 42, 177-184.

Siregar, P., Le Noach, R., Scarabin, J.M., Coatrieux, J.L., 1989. Problème inverse et stabilité en électroencéphalographie. Innov. Tech. Biol. Med. 10(6), 643-658.

Siregar, P., Mabo, P., Coatrieux, J.L., 1993. How can deep knowledge be used in CCU Monitoring? Special Issue on Intelligent Monitoring Systems, IEEE Eng. Med. Biol., 4(12), 92-99.

Siregar, P., Sinteff J.P., 1996b. Introducing spatio-temporal reasoning into the inverse problem in electroencephalography. Artif. Intell. Med., 8, 97-122.

Siregar, P., Sinteff, J.P., Julen, N., Le Beux, P., 1997. Spatio-Temporal Reasoning For Multi-scale Modeling in Cardiology. Special Issue on Cardiovascular Systems, Artif. Intell. Med. 10, 41-57.

Siregar, P., Sinteff, J.P., Julen, N., Le Beux, P., 1998. An interactive 3D anisotropic cellular automata model of the heart. Comput. Biomed. Res. 31, 323-347.

Siregar, P., Sinteff, J.P., Lemoulec, F., Le Beux P., 1996c. A Cellular Automata of the Heart and its coupling with a Qualitative Model. Comput. Biomed. Res. 29(3), 222-246.

Siregar, P., Toulouse, P., 1995. Model-based Diagnosis of Brain Disorders: A Prototype Framework. Artif. Intell. Med. 7(4), 315-342.

Strilic, B., Eglinger, J., Krieg, M., Zeeb, M., Axnick, J., Babal, P., Muller, D.J., Lammert, E., 2010. Electrostatic cell-surface repulsion initiates lumen formation in developing blood vessels. Curr. Biol. 20, 2003-2009.

Takasato, M., Er, P.X., Chiu H.S., Maier, B., Baillie, G.J., Ferguson, C., Parton, R.G., Wolvetang, E.J., Roost, M.S., Lopes, S.M., Little, M.H., 2015. Kidney organoids from human iPS cells contain multiple lineages and model human nephrogenesis. Nature 526, 564-568. https://doi:10.1038/nature15695.

Tallinen, T., Chung, J.Y., Biggins, J.S., Mahadevan, L., 2014. Gyrification from constrained cortical expansion. Proc. Natl. Acad. Sci. U.S.A, 111(35), 12667-12672.

Tanaka, M., 2016. Developmental Mechanism of Limb Field Specification along the Anterior–Posterior Axis during Vertebrate Evolution. J. Dev. Biol. 4:18. https://doi:10.3390/jdb4020018.

Teague, B.P., Guye, P., Weiss, R., 2016. Synthetic Morphogenesis. Cold Spring Harb. Perspect. Biol. 8(9). pii: a023929. https://doi: 10.1101/cshperspect.a023929.

Ten Tusscher, K.H., Noble, D., Noble, P.J., Panfilov A.V., 2004. A Model for Human Ventricular Tissue. Am. J. Physiol. Heart Circ. Physiol. 286, H1573-H1589. https://doi.org/10.1152/ajpheart.00794.2003.

Torquato, S., 2011. Toward an ising model of cancer and beyond. Phys. Biol. 8(1), 015017. https://doi.org/10.1088/1478-3975/8/1/015017.

Trepat, X., Fredberg, J., 2011. Plithotaxis and emergent dynamics in collective cellular migration. Trends Cell Biol. 21(11), 638–646.

Turing, A.M., 1952. The chemical basis of morphogenesis. Philos. Trans. R. Soc. Lond. B Biol. Sci. 237(641), 37-72.

Urban, A.E., Zhou, X., Ungos, J.M., Raible, D.W., Altmann, C.R., Vize, P.D., 2006. FGF is essential for both condensation and mesenchymal-epithelial transition stages of pronephric kidney tubule development. Dev. Biol. 297, 103–117.

Varner, V.D, Nelson, C.M, 2014. Cellular and physical mechanisms of branching morphogenesis. Development 141, 2750-2759.

Varner, V.D, Taber, L.A., 2012. On Integrating Experimental and Theoretical Models to Determine Physical Mechanisms of Morphogenesis. Biosystems, 109(3), 412–419.

Versteeg, H.H., Johan, W.M., Heemskerk, J.W.M, Levi, M., Reitsma, P.H., 2013. New fundamentals in hemostasis. Physiol. Rev. 93, 327–358.

Vize, P., Woolf, A., Bard, J., 2003. The Kidney: From Normal Development to Congenital Diseases. Academic Press, Amsterdam.

Walck-Shannon, E., Hardin, J., 2014. Cell intercalation from top to bottom. Nature Rev. Mol. Cell Biol. 15, 34–48.

Wang, R.N., Green, J., Wang, Z., et al. 2014. Bone Morphogenetic Protein (BMP) signaling in development and human diseases. Genes Dis. 1(1), 87-105.

Wang, S., Sekiguchi, R., Daley, W.P., Yamada K.M., 2017. Patterned cell and matrix dynamics in branching morphogenesis, J. Cell Biol. 216, 559-570.

Wang, Y., Wang, X., Wohland, T., Sampath, K., 2016. Extracellular interactions and ligand degradation shape the nodal morphogen gradient, eLife 5:e13879. https://doi:10.7554/eLife.13879.

Weaver, M., Dunn, N.R., Hogan, B.L.M., 2000. Bmp4 and Fgf10 play opposing roles during lung bud morphogenesis. Development 127, 2695-2704.

Wittmann, D.M., Krumsiek, J., Saez-Rodriguez, J., Lauffenburger, D.A., Klamt, S., Theis, F.J., 2009. Transforming Boolean models to continuous models: methodology and application to T-cell receptor signaling. BMC Systems Biology 3:98.

Wolfram, S., 2002. A New Kind of Science. Wolfram Media Inc.

Wolpert, L., Beddington, R., Jessell, T., Lawrence, P., Meyerowitz, E., Smith J., 2002. Principles of Development, Second Edition Oxford University Press ISBN 0-19-924939-3.

Yamaguchi, S.K.M., Yoshimoto, E., 2007. Pattern regulation in the stripe of zebrafish suggests an underlying dynamic and autonomous mechanism. Proc. Natl. Acad. Sci. U.S.A. 104, 4790-4793.

Yu, S.R., Burkhardt, M., Nowak, M., Ries, J., Petrásek, Z., Scholpp, S., Schwille, P., Brand, M., 2009. FGF8 morphogen gradient forms by a source-sink mechanism with freely diffusing molecules, Nature 461, 533-536.

Zienkiewicz, O.C., Taylor, R.L., Nithiarasu, P., 2005. The finite element method for fluid dynamics. Elsevier ed.

7. Figures

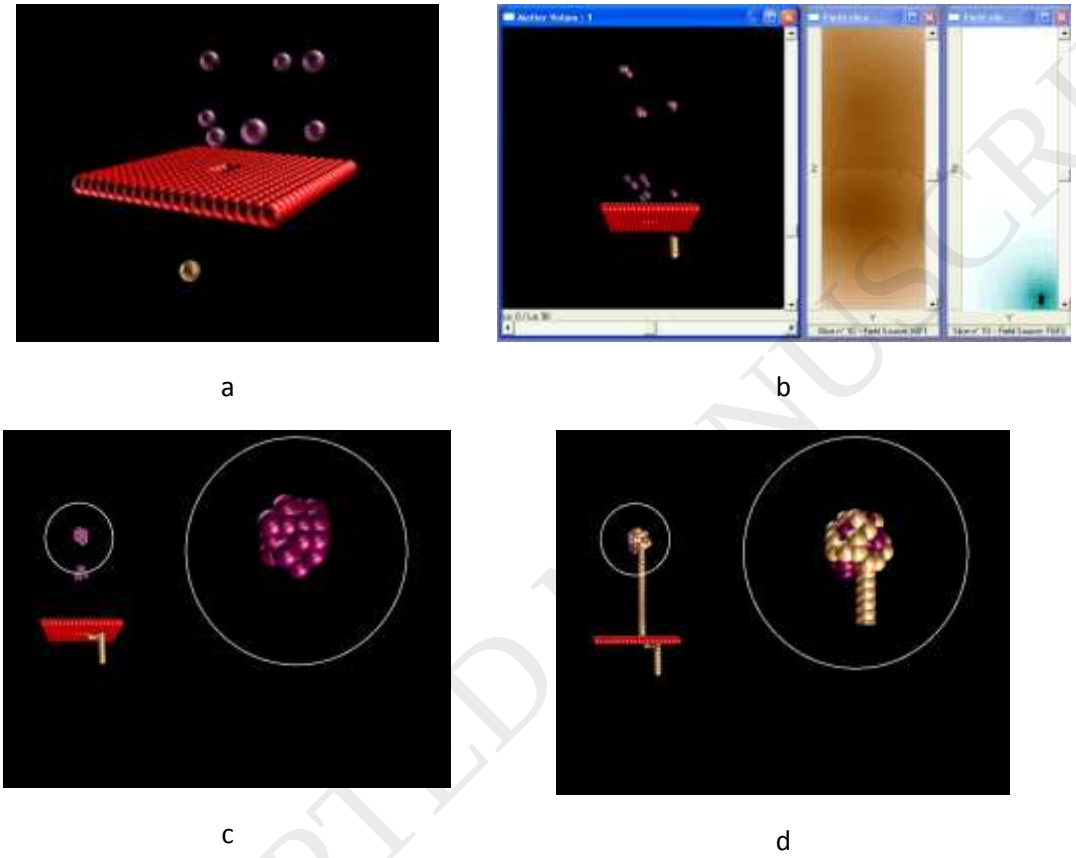

Figure 1. Morphogenesis: simulation of an imaginary example

This is an imaginary three-signal (IGF1, FGF2, Semaph) scenario that was designed to simulate many of the concepts described in this paper: *progenitor cell*, *cell lineage*, *cell state*, *mutual induction*, *paracrine inhibition*, *autocrine positive feedback*, *chemotaxis*, *morphogen gradient*, *repulsive semaphorins*, *lateral inhibition*, *oriented cell division*, *elongation*, *collective cell migration*, *condensation*, *vesicle formation, cell fate*.

Fig. 1a. The initial conditions. Two distinct populations of progenitor cells leading to two distinct cell lines are separated by a barrier that has a rectangular hole at its center. The initial yellow-coded cells are progenitors of “duct epithelial” cells and the purple-coded cells are progenitors of “vesicle epithelial” cells.

Fig. 1b. Mutual induction: "vesicle progenitor" cells progenitor (state 0), secrete IGF1 (the name is really not important here), that induce "duct progenitor" cells to become (state 1) "duct" cells. Duct cells in state 1 secrete FGF2 which induces "vesicle progenitor" cells to become to state 1 "duct" cells. IGF1 acts as an autocrine signal for (state 1) vesicle cells and promotes vesicle cell mitosis, collective migration and aggregation (positive feedback). IGF1 also acts as a paracrine signal for (state 1) duct cells that proceeds to oriented cell division and elongation following a positive IGF1 gradient. Also, the duct tip cells (state 1), proceed to asymmetric cell division insofar as the most distal cell remains in state 1 while the more proximal one is a (state 2) duct cell that expresses a receptor for FGF2. FGF2 acts as a lateral inhibitor for (state 2) duct cells preventing them to form branches.

Fig. 1c. FGF2 acts as a paracrine repulsive and anti-mitotic signal for (state 1) vesicle cells. That is, (state 1) vesicle cells move away from the duct cells in the direction of a negative FGF2 gradient. FGF2 also acts as an instructive signal insofar as vesicle cells distal to the FGF2 source divide more rapidly than those closer to the source. Finally, the cells of the rectangular structure secrete a short-range semaphorin, that induces an avoidance behavior from the "duct" cell. Oriented cell division then integrates two cues, the IGF1 gradient and the short-range semaphoring repulsion allowing the "duct" cells to find the hole and proceed towards the "vesicle" cells.

Fig. 1d. All active vesicle cells have finally condensed into a packed ball of cells. Due to their proximity, short range repulsion equilibrates the chemical attraction. As the "duct" cells come in contact with, and surround the vesicle cells, they induce the vesicle cells to switch from an active state to a quiescent one. Quiescent vesicle cells cease to produce IGF1 and all migratory and mitotic activity of both "vesicle" and "duct" cells is stopped. A stable two cell-type structure has been formed.

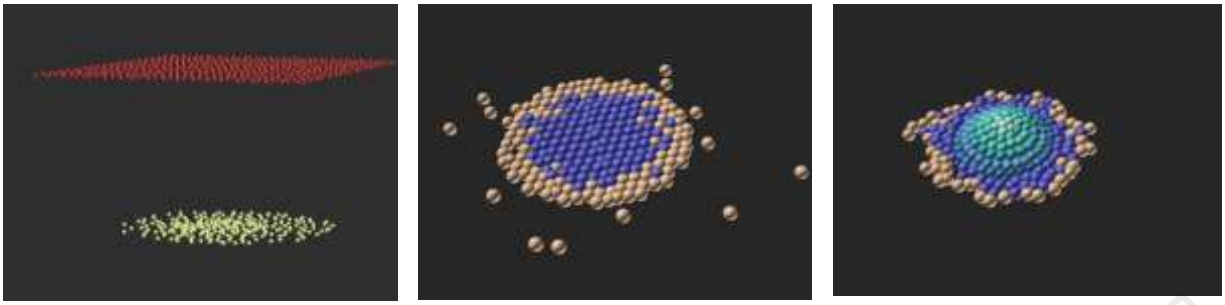

a b c

Figure 2. **Cell migration, condensation, differentiation, and budding.**

Fig. 2a. General setting between metanephric mesenchyme (MM) inductor cells (color-code = red) and collecting duct (CD) progenitor cells (color-code = yellow). The initial conditions are as follows. The MM inductor cells secrete GDNF and the (CD) progenitors express the GDNF receptors RET.

Fig. 2b. Mutual induction, permissive induction and condensation of the ureteric progenitor cells. Initiation consists of the mutual induction between ($GDNF^+$, SIX^+) mesenchyme cells and (RET^+, $WNT11^+$) CD progenitors. CD formation are induced by the secretion of GDNF by the ($GDNF^+$, SIX^+) mesenchyme cells resulting in the activation of the CD progenitors (fig. 2a). Once a GDNF concentration threshold is reached, CD progenitors become activated and secret Wnt9b as well as a hypothetic autocrine factor FX (we hypothesized this signal). Wnt9b induces the MM cells to maintain their secretion of GDNF while the autocrine factor FX plays the role of a chemoattractant for CD progenitors. As a result, activated CD progenitors migrate and condense in the direction of the FX gradient which corresponds to the direction of the center of the combined cell mass. Cells within the condensate that sense a concentration of FX above a threshold differentiates into an immature CD epithelial cell (color-code=blue).

Fig. 2c. Instructive induction, collective migration and budding. The immature CD cells express RET and FX receptors. In addition to its role in condensation, FX plays an instructive inductive role in which the states of the immature CD epithelial cell become differentiated as follows. All cells self-organize according to the FX concentration that they sense. The cells that sense the highest FX concentration become the lead tip cells and have the highest RET expression while the remaining cells self-organize into concentric iso-RET (reminiscent of isopotentials) expression groups from which ureteric budding can be initiated Cells belonging to the same iso-RET expression group will behave the same way (e.g. speed of migration) when subject to the same conditions. In this example, immature CD cells migrate “upwards” in the scene by following the GDNF concentration gradient secreted by the MM cells (fig. 3a). Finally, inactive cells (light orange) will undergo apoptosis.

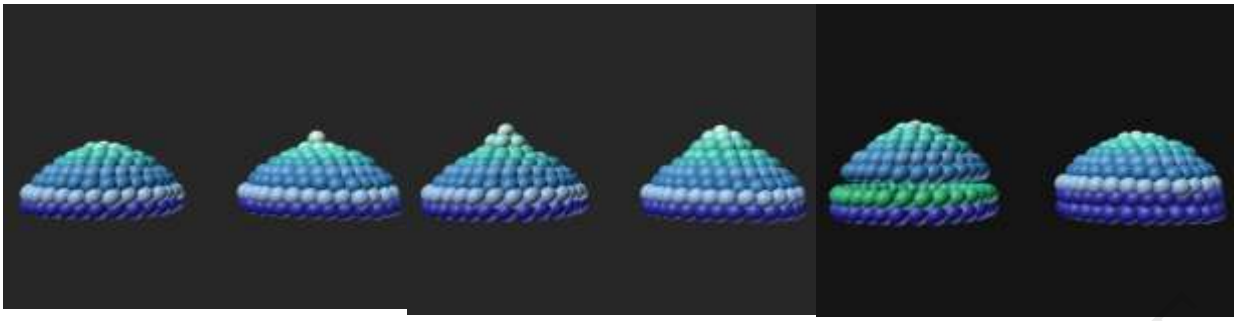

a b c

Figure 3. **Oriented cell division and elongation.**

In one of our model, the elongation of the ureteric bud proceeds by cycles.

Figs 3a-3b. Migration speed, if unhindered, decreases as we proceed from the central tip cells to the more peripheral ones hence at the start of each cycle, central cells move faster than peripheral ones. However, since cells are mechanically linked, the slower moving cells get an additional pull forward from leading cells while the latter are pulled backward resulting in a propagating longitudinal wave of contraction expansion that starts at the tip. This simulation illustrates one of our modeling simplifications in which the grey-coded (RET^+, $WNT11^+$) cells, one row above the bottom, (RET^- $WNT11^-$) epithelial cells (dark blue), are the only UB cells that can divide during elongation.

Fig. 3c. When the pulling force perceived by a (RET^+, $WNT11^+$) grey-coded cell exceeds a threshold, it changes state (green), divides asymmetrically and in the direction of the main axis following planar cell polarity. One of the daughter cell is also a (RET^+, $WNT11^+$) CD progenitor (grey) and the other is a (RET^- $WNT11^-$) UB trunk cell (dark blue) that contributes to the lengthening of the UB trunk epithelial lining (dark blue). Trunk epithelial cells become quiescent and in order to reduce the computational load, their dynamic parameters, properties, and procedural attachments are deleted from the corresponding C++ objects. This, however, is another simplification since in reality even “inactive” cells are under constant mechanical stress and thus kinematic variations.

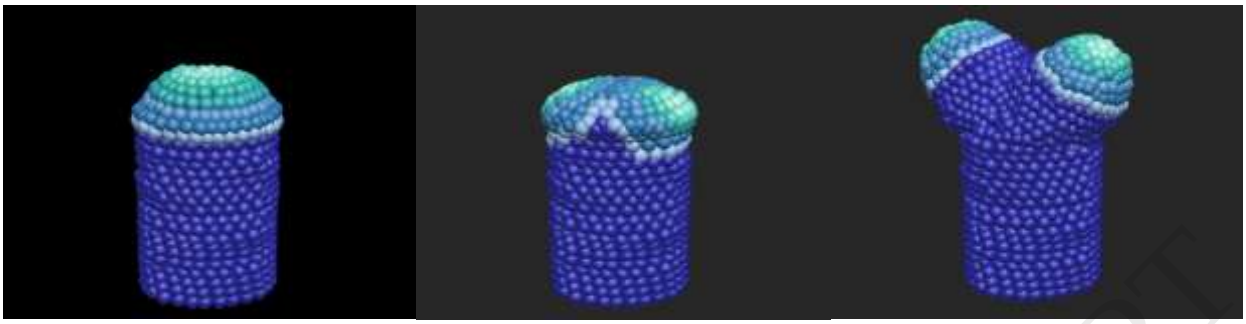

a b c

Figure 4. Branching.

Branching follows phenomenological rules.

Fig. 4a. At each elongating cycle, the active leading bulge or ampulla flattens. UB flattening can be obtained in a number of ways. In our models it can be due to a concentric RET-dependent differential of cell proliferation or due to the fact that the rate-of change of central cells' migration velocity decreases faster than the more peripheral ones.

Fig. 4b. When a "flatness" threshold is reached, the current tip cells become (RET^+, $WNT11^+$), and two new tip cells positioned at the periphery are selected as follows: they belong to the same iso-RET group, they are opposite to each other with respect to the main axis, and they are chosen "by vote" according to the lowest levels of semaphorin concentrations. Indeed, since all cells (and thus growing structures) produce semaphorins, the lowest local semaphorin levels will indicate more "free space" in these directions. The new selected tip cells secrete factor FX and the RET expressions are re-adjusted accordingly.

Fig. 4c. Two new concentric iso-RET patterns are formed thus initiating two elongation processes.

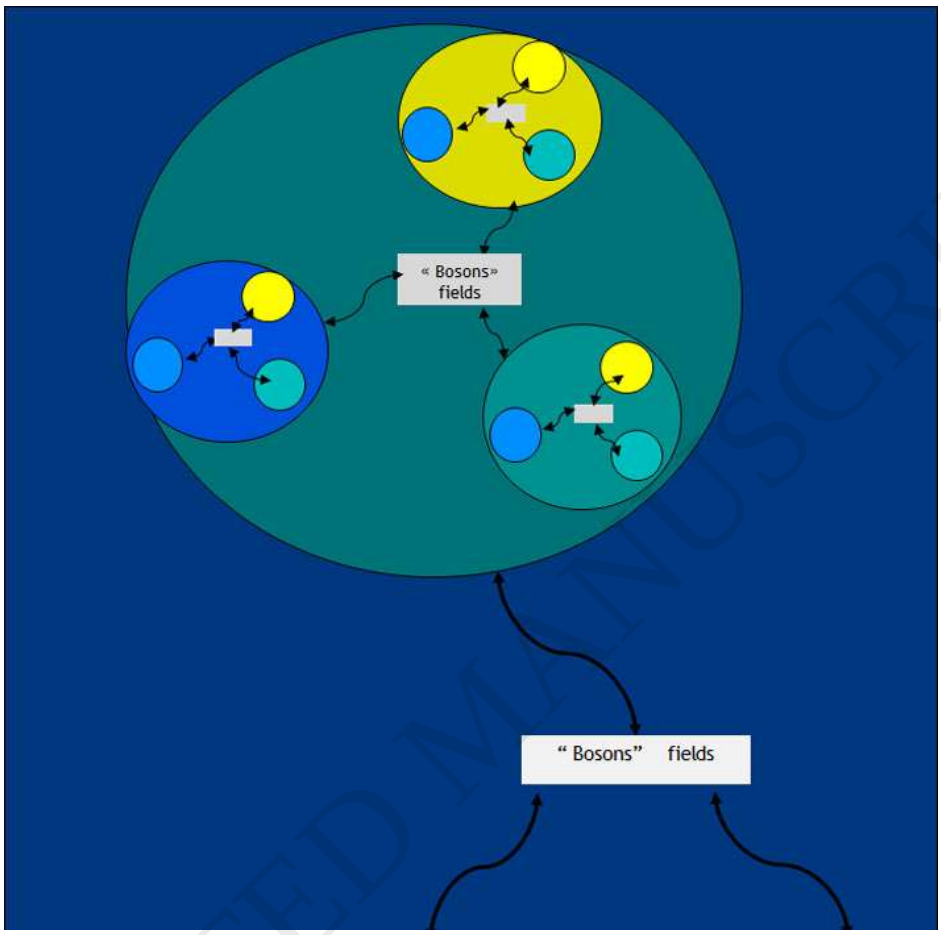

Figure 5. General GMSP architecture. The GMSP’s general architecture was inspired by fundamental physics in which matter (fermions) interacts via bosons. Any system is defined as an agent that may (recursively) be composed of sub-units that are also agents in interaction with each-other. Thus at each level of description, agents are embodied/situated within a network of dynamic interactions.

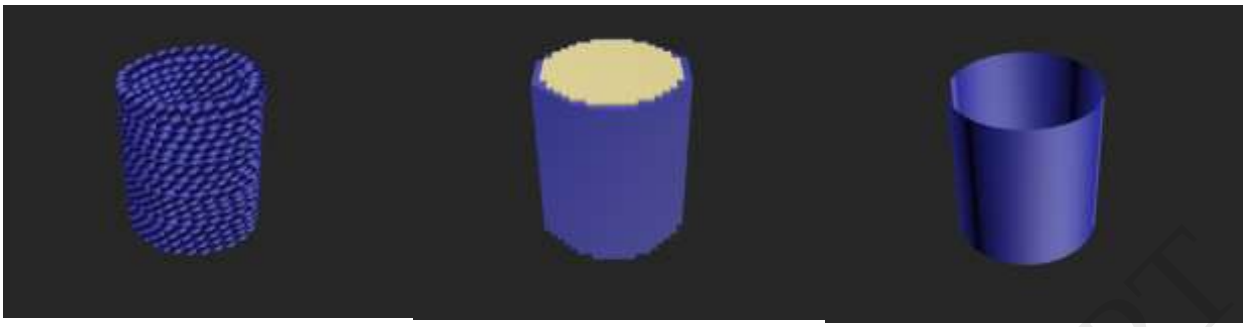

a b c

Figure 6. **The different 3D models.**

Fig. 6a. Lattice-free representation. An UB wall generated during the morphogenetic process.

Fig. 6b. Grid representation. During morphogenesis, voxel/regular grid spaces are segmented into domains. Each voxel is assigned a label that defines a domain. In this example, the UB wall and lumen are computed from the data obtained from the lattice-free object following procedures described in (Siregar, 2000, 2009). In our current version, some physical processes such as diffusion are modeled using grid-based finite-difference methods while others, e.g. mechanical and cell kinematics, follow a lattice-free SPH approach. The voxel/lattice assignment varies between time points as cells may differentiate, die, or migrate. Each voxel/lattice is thus re-assigned new labels as morphogenesis proceeds. Thus at any point in time during simulation, the entire voxel/grid space is re-partitioned into closed sub-domains.

Fig. 6c. Polygonal representation. Each generated volumetric model can be converted into smooth tissue boundary polygonal surface models that are more amenable to visual interpretation. It's also an element of our multi-scale modeling toolkit that has a smoothing effect as we proceed from one mesh resolution to a finer one. More will be said about this important issue in some future paper.

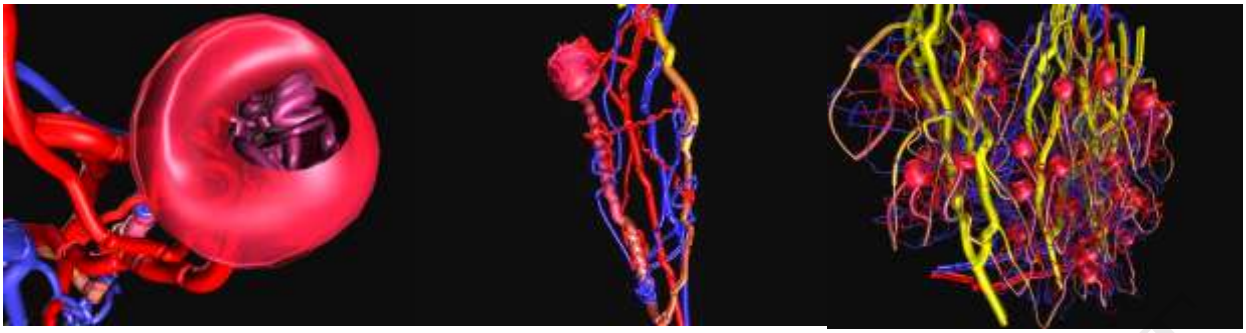

a b c

Figure 7. Multi-scale polygonal representations of generated kidney structures

The morphogenic concepts explained therein have also been applied to nephron and vessel generation. For instance, vessel progenitor cells dispersed within the mesenchyme become activated, migrate and proliferate under the influence of VEGF that are secreted by active immature epithelia.

Fig. 7a. Bowman's capsule and nephron glomerulus with afferent and efferent arterioles.

Fig. 7b. A single nephron functional unit that includes afferent and efferent arterioles, venules and a collecting duct segment.

Fig. 7c. Multiple nephrons with arcuate artery and vein.